

North American Actuarial Journal

ISSN: (Print) (Online) Journal homepage: https://www.tandfonline.com/loi/uaaj20

Storm CAT Bond: Modeling and Valuation

Shimeng Huang, Jinggong Zhang & Wenjun Zhu

To cite this article: Shimeng Huang, Jinggong Zhang & Wenjun Zhu (06 Oct 2023): Storm CAT Bond: Modeling and Valuation, North American Actuarial Journal, DOI: 10.1080/10920277.2023.2226734

To link to this article: https://doi.org/10.1080/10920277.2023.2226734

© 2023 The Author(s). Published with license by Taylor & Francis Group, LLC

View supplementary material

Published online: 06 Oct 2023.

Submit your article to this journal

Article views: 20

View related articles

View Crossmark data

Full Terms & Conditions of access and use can be found at https://www.tandfonline.com/action/journalInformation?journalCode=uaaj20

North American Actuarial Journal, 0(0), 1–26, 2023
© 2023 The Author(s). Published with license by Taylor & Francis Group, LLC
ISSN: 1092-0277 print / 2325-0453 online
DOI: 10.1080/10920277.2023.2226734

Routledge
Taylor & Francis Group

OPEN ACCESS Check for updates

Storm CAT Bond: Modeling and Valuation

Shimeng Huang,[1] Jinggong Zhang,[2] and Wenjun Zhu[2]
[1]*Department of Risk and Insurance, Wisconsin School of Business, University of Wisconsin–Madison, Madison, Wisconsin*
[2]*Division of Banking & Finance, Nanyang Business School, Nanyang Technological University, Singapore*

The frequency and intensity of weather-related catastrophes, such as storms and floods, have been increasing due to climate change. This leads to rising storm catastrophe risks to the property–casualty insurance and reinsurance sector. In this article, we propose an index-based storm catastrophe (CAT) bond for reinsurers to hedge catastrophe risks related to storm losses. Storm loss data have a large portion of zero values and a continuous positive right-skewed distribution, together with high-dimensional spatial dependence. We address these unique properties by proposing a general two-part autoregressive (2PAR) distribution as the marginal model and a semicontinuous spatiotemporal vine copula as the dependence model. We investigate the CAT bond market equilibrium and endogenously solve for the optimal market price of risk and coupon rates. Our empirical results using historical loss data at the county level in Florida show that the proposed CAT bond can stabilize the reinsurer's cash flows and create attractive returns to investors by offering high coupon rates. Our framework can be generalized to design and price other catastrophe financing facilities.

1. INTRODUCTION

Natural disasters, although infrequent, may lead to catastrophic events and cause substantial financial losses. For example, losses from Hurricane Andrew in 1992 amounted to US$26.5 billion, and Hurricane Katrina, the costliest hurricane in U.S. history, led to losses of approximately US$75 billion in the New Orleans area and along the Mississippi coast (National Hurricane Center). In particular, weather-dependent losses have become the predominant driver of catastrophe insurance losses (Mills 2005). Climate change such as global warming has increased both the frequency and intensity of weather-related disasters, such as storms (Coronese et al. 2019). Evidence has shown a rising frequency of storm events in recent decades (Dunstone et al. 2013; Murakami et al. 2020). As a result, economic losses due to weather-related catastrophe events like storms and floods have been dramatically increasing over the years (Hoeppe 2016; Coronese et al. 2019). In fact, insured property losses are dominated by storm events—more than 70% of US$374 billion insured property losses from 1980 to 2004 was due to storms (Mills 2005), and US$81 billion of natural catastrophe insured losses in 2019 was mostly inflicted by severe convective storms (Swiss Re Institute 2021). The property and casualty (re)insurance sector is highly focused on managing extreme losses due to natural disasters (Priest 1996; Odening and Shen 2012), and, hence, is facing more pronounced losses due to additional exposure to catastrophe losses resulting from increased climate variability in the future. Mills (2005) listed eight challenges in modeling catastrophe losses, including shortening times between loss events, changing the spatial distribution of events, and abrupt changes in losses. Aon's report also concluded that catastrophic events will increase in ways that are impossible to predict using conventional risk assessment methods (Aon 2021). Therefore, exploring innovative approaches for catastrophe loss prediction and risk sharing is essential to be better prepared for future challenges.

Address correspondence to Wenjun Zhu, Division of Banking & Finance, Nanyang Business School, Nanyang Technological University, Singapore 639798. E-mail: wjzhu@ntu.edu.sg

Supplemental material for this article can be accessed on the publisher's website at www.tandfonline.com/uaaj.

This is an Open Access article distributed under the terms of the Creative Commons Attribution-NonCommercial-NoDerivatives License (http://creativecommons.org/licenses/by-nc-nd/4.0/), which permits non-commercial re-use, distribution, and reproduction in any medium, provided the original work is properly cited, and is not altered, transformed, or built upon in any way. The terms on which this article has been published allow the posting of the Accepted Manuscript in a repository by the author(s) or with their consent.

Property–casualty insurance companies usually transfer catastrophe risk with reinsurance. However, this diversification might not be sufficient, leading to insolvencies of insurers and reinsurers, especially given the dramatic increases in catastrophe losses over recent years. Charpentier (2008) concluded that climate risks, especially natural catastrophes, are hardly insurable. Cummins, Doherty, and Lo (2002) showed that there would be billions of dollars in unpaid claims and a large number of insurer insolvencies following a mega-catastrophe despite the increasing ability of insurers to manage catastrophe risks. Niehaus (2002) identified moral hazard and adverse selection problems as the market imperfections that limit sufficient diversification of catastrophe risks and thus limit the ability of insurers and reinsurers to pay catastrophe claims. Froot (1999) concluded that catastrophic event risk distribution is inefficient, and Froot (2001) provided eight theoretical explanations, including behavioral explanations and price regulation at the state level, for the limited sharing of catastrophe risk. Moreover, on the supply side, using a model for catastrophic risk markets, Ibragimov, Jaffee, and Walden (2009) explained why (re)insurers provide limited protection against catastrophic risk that leads to a" nondiversification trap."

As a result, to achieve more efficient risk sharing and better risk management strategies, capital market solutions to hedge catastrophe risks with innovative financial instruments, such as contingent capital, catastrophe (CAT) futures and options, CAT swaps, as well as CAT bonds, have become important complementary approaches to traditional reinsurance (e.g., Doherty 1997; Froot 1999; Cummins, Lalonde, and Phillips 2004; Nell and Richter 2004; Golden, Wang, and Yang 2007; Charpentier 2008; Cummins 2008; Cummins and Trainar 2009; G. Wang and Wang 2019; X. Wang 2019; Götze and Gürtler 2022). In particular, CAT bonds are by far the most popular and successful hedging instrument in the market due to their high yields and low correlations with the financial market returns. They are attractive to investors as a risk diversification tool (Cummins 2008; Braun 2016). For example, as of 2020, catastrophe bonds and insurance-linked securities issued and outstanding were $14.17 billion and $46.36 billion, respectively.[1] In a CAT bond agreement, investors forgive some principal and/or coupon payments if a specific catastrophe takes place. In this case, the coupon/principal payout retained may help to stabilize the bond issuer's cash flows during natural disasters. If no catastrophe occurs, investors receive their principal plus coupons that are much higher than LIBOR (Froot 2001; Niehaus 2002). Thus, a CAT bond arrangement can potentially benefit both the bond issuer and investors.

In this article, we focus on the problem of securitization for storm CAT risk sharing between reinsurers and the capital market. This article proposes an index-based storm CAT bond for reinsurers to hedge risks related to property losses due to storm events (hereafter "storm loss(es)"). Motivated by the incomplete nature of the storm CAT bond market, we take a market equilibrium approach to derive CAT bond prices by taking into account the risk preferences of both supply and demand sides. In particular, we endogenously determine the equilibrium market price of risk, issue size, and coupon rates based on the bond issuer's and buyer's optimal terminal wealth conditions. The statistical modeling of underlying risks is essential in both the supply and demand sides of the market (Campbell and Diebold 2005). Therefore, this research refines the statistical modeling of storm losses and addresses the challenges of storm CAT bond modeling in an incomplete market. In particular, we propose to use a general two-part autoregressive (2PAR) model as the marginal distribution of the longitudinal storm losses and employ a semicontinuous spatiotemporal vine copula approach to incorporate dependence into the storm CAT bond valuation. Results of empirical analysis using historical storm loss data in the state of Florida show that the proposed statistical framework is capable of capturing the storm loss characteristics, and the proposed storm CAT bond can stabilize the reinsurer's cash flows and create attractive returns to investors in the capital market.

In developing an effective storm CAT bond structure and pricing framework, the statistical modeling of storm losses is essential yet challenging, owing to some unique characteristics of longitudinal storm loss data. In particular, storm loss data have a large number of zero values and a continuous positive right-skewed distribution. Moreover, storm losses are often high-dimensional with significant spatial dependence. Zero values are present when no storm event occurs or when storm events cause no property losses. In this article, we propose a general 2PART model as the marginal distribution of the longitudinal storm losses. The two-part model, introduced by Aitchison (1955), combines a binary model and a positive continuous model. It is commonly used to model semicontinuous distributions. For example, Duan et al. (1983) and Manning et al. (1981) used the two-part distribution for medical expenditures, and Shi and Yang (2018) adopted the two-part distribution to model insurance claims. Y. Wang, Wang, and Zhuang (2018) extended the original two-part model by incorporating an autoregressive process. The general 2PAR model we develop in this article is a flexible extension of Y. Wang, Wang, and Zhuang (2018), which relaxes the choice of positive continuous distributions. The resulting general 2PAR model better captures the property of storm losses because it not only accounts for the semicontinuous feature and the serial correlation of the storm loss time series but also captures the right skewness and heavy tails of storm losses.

[1]Source: Artemis Catastrophe Bond & Insurance-Linked Securities Deal Directory (https://www.artemis.bm).

The copula is a class of flexible and convenient models to capture the dependence structure of high-dimensional random variables.[2] It has been widely used and investigated in the actuarial and insurance studies (see, e.g., Frees and Valdez 1998, 2008; Klugman and Parsa 1999; Juri and Wüthrich 2002; Frees and Wang 2005; Cossette, Marceau, and Marri 2008; Genest, Rémillard, and Beaudoin 2009; Okhrin, Odening, and Xu 2013; Shi, Feng, and Boucher 2016; Su and Hua 2017; Zhu, Tan, and Wang 2017; Zhu et al. 2018; Zhou and Ji 2021). There is a growing body of literature exploring spatiotemporal dependence modeling using copulas. For example, Zhao, Shi, and Feng (2021) employed a novel copula model to accommodate the spatial and temporal dependence among spatially clustered property risks. This proposed copula-based framework allows insurers to learn from experience of related risk cohorts along with the policyholder's own history. The authors also proposed a multilevel composite likelihood approach to reduce the computational burden due to high dimensionality. To model tail dependence and tail asymmetry, Krupskii and Genton (2017) and Krupskii, Huser, and Genton (2018) developed a factor copula model for replicated spatial data, assuming a common factor exists and affects the joint dependence of all measurements in space and in time. Another popular strand of literature on spatial dependence employs vine copulas (see, e.g., Gräler 2014; Erhardt, Czado, and Schepsmeier 2015a,b). Vine copula model addresses the challenge of high dimensionality through simple building blocks of bivariate copulas and pair copula constructions (Joe and Xu 1996; Bedford and Cooke 2002; Kurowicka and Cooke 2006; Aas et al. 2009). Following this line of literature, we propose to employ a parsimonious yet flexible semicontinuous spatiotemporal vine copula structure to model the dependence among storm losses over space and time, by extending the model developed by Gräler and Pebesma (2012) and Gräler (2013, 2014). This approach is simple with the separating distance as the only parameter that controls the strength of dependencies. Through convex combinations of bivariate copulas, the spatiotemporal vine structure provides flexibility in the selection of bivariate copula families and thus is able to capture non-Gaussian dependence structures. In particular, to accommodate the semicontinuous feature of storm losses, we further extend the continuous model in Gräler and Pebesma (2012) and Gräler (2013, 2014) using a mixed vine approach introduced by Shi and Yang (2018).

Our contribution to the literature is twofold. First, from the statistical modeling perspective, we develop a parsimonious and flexible multidimensional framework to accommodate serial correlation and spatiotemporal dependence for semicontinuous storm loss data with a fraction of zero values. Existing studies of CAT bond pricing mostly focus on the theoretical development of bond pricing at the expense of practical applications (Karagiannis et al. 2016). It is crucial to consider the distributions of the underlying CAT risks because there are unique characteristics of different types of CAT risks, and the statistical modeling of underlying risks is essential in both the supply and demand sides (Campbell and Diebold 2005). As discussed earlier, owing to the incompleteness of the CAT bond market, we price the proposed storm CAT bond using the market equilibrium approach, by taking into account both the demand and supply of the CAT bond. One typical storm risk feature that makes the supply-side analysis challenging is its high geographical dependence. For example, when a major hurricane hits, a reinsurer will likely receive claims from insurers at different locations impacted by the same event. As discussed in Cummins and Trainar (2009), risk securitization becomes increasingly important when the correlation among risks increases. Therefore, if the dependence is incorrectly specified or modeled, the optimal quantity of the CAT bond issuance and, hence, the market price will be misidentified. However, the dependence structure of CAT risks has yet been studied comprehensively in the CAT bond pricing literature. To better incorporate this key element into storm CAT bond valuation, we propose a general 2PAR model as the marginal distribution of the longitudinal storm losses and employ a semicontinuous spatiotemporal vine copula approach to incorporate dependence into the storm CAT bond valuation. Our empirical results highlight the importance of dependence modeling in CAT bond valuation, because an incorrect independence assumption will lead to suboptimal hedging strategies.

Second, from the CAT bond pricing perspective, we develop a CAT bond pricing framework in the incomplete market using market equilibrium. The storm CAT bond market is incomplete and, thus, there is no universal pricing theory or unique pricing measure that successfully deals with all aspects of pricing (Young 2004; Karagiannis et al. 2016), and it is not always possible to rely on existing securities to calibrate the market price of risk. As a result, various interesting pricing methods have been explored in the literature. Some early works treated CAT bonds as zero-beta securities by assuming a zero risk premium for CAT risks (Cummins and Geman 1995; Cox, Fairchild, and Pedersen 2000; Cox and Pedersen 2000; Lee and Yu 2002, 2007). In particular, Lee and Yu (2002) incorporated stochastic interest rates and allowed for moral hazard, basis risk, and default risk, and Lee and Yu (2007) adopted this approach to investigate the impact of CAT bond issuance on reinsurers. A large number of works on the pricing of CAT bonds and derivatives are based on preference free no-arbitrage frameworks (see, e.g., Muermann 2008; Jarrow 2010; Braun 2011; Nowak and Romaniuk 2013). Vaugirard (2003) was the first to develop a simple arbitrage approach to evaluate CAT risk securities and vindicate the existence of arbitrage prices for CAT bonds based on a risk index. Nowak and Romaniuk (2013) extended this approach, and Braun (2011) developed a two-stage contingent claims pricing approach to price CAT swaps. First introduced by Hodges and Neuberger (1989), utility indifference pricing is another approach widely used in the literature (see, e.g., Young 2004; Egami and Young 2008; Karagiannis et al. 2016). This approach applies the principle of equivalent utility to calculate the price at which the issuer of the security is indifferent

[2]For an introduction to copula models, see, for example, Nelsen (2007) and McNeil, Frey, and Embrechts (2015).

in terms of her expected utility of the optimal terminal wealth. Moreover, S. S. Wang (1996, 2000, 2002) developed a class of probability transforms, the Wang transform, to price securities in an incomplete market. It has been widely used in CAT bond pricing literature (see, e.g., Lin and Cox 2005, 2008; Denuit, Devolder, and Goderniaux 2007; Chen and Cox 2009; Chen and Cummins 2010; Galeotti, Gürtler, and Winkelvos 2013; Tang and Yuan 2019). Galeotti, Gürtler, and Winkelvos (2013) compared different premium calculation models and found that the Wang transform has consistently accurate predictive power. In addition, the econometric pricing model has become increasingly popular to identify the factors that determine CAT bond premium and price of the bond (Braun 2016; Gürtler, Hibbeln, and Winkelvos 2016; Götze and Gürtler 2020). Unfortunately, much of the existing research focused on CAT bond pricing from the perspective of bond issuers. However, both issuers and buyers play important roles in the market of CAT bonds (Campbell and Diebold 2005). CAT bond pricing without considering buyers' risk preferences on the demand side may lead to a demand and supply mismatch, as documented by Evans (2022). Therefore, by considering both the demand and supply of CAT bonds in this article, we bring the trade-off analysis to the attention of CAT bond research. We derive CAT bond prices based on market equilibrium by taking into account the risk preferences of both the bond issuer and buyer. In particular, we use the equivalent martingale measure identified by the Wang transform (S. S. Wang, 1996, 2000, 2002) and endogenously determine the equilibrium market price of risk, issue size, and coupon rates based on the bond issuer's and buyer's optimal terminal wealth conditions. This article provides guidance and insights into future design and pricing of CAT bonds and other catastrophe financing facilities.

Finally, whereas reinsurers are more practically concerned about losses above the reinsurance deductible, this article focuses on modeling the entire data-generating process of storm losses rather than just truncated or censored data, for three reasons. First, the article aims to model the dynamics of the entire storm CAT bond market, including all three parties involved: insurers, the reinsurer, and the investor. Losses below the deductible are important for the framework of CAT bond design and pricing because insurers' losses are related to reinsurance contracts and ceded losses, affecting the proposed storm CAT bond. Second, in practice, the deductibles and policy limits of reinsurance contracts are subject to variation across different insurers and over time, which affects the ceded losses to the reinsurer and CAT bond pricing. Finally, modeling the whole data-generating process with the entire sample will increase the sample size and hence improve the statistical soundness of modeling. Modeling truncated or censored losses due to deductibles is challenging because loss amounts below thresholds also contain valuable information, and the insured may choose deductible levels based on their hidden risks (e.g., Shi and Lee 2022). Therefore, the article avoids such challenges by directly modeling the entire data-generating process of storm losses.

The remainder of this article is organized as follows. Section 2 presents the modeling methodology including marginal and dependence models for storm losses. Section 3 describes the structure and market of the storm CAT bond and introduces the pricing framework. In Section 4, we present an empirical study using storm losses in the state of Florida. The pricing results are summarized in Section 5. Section 6 concludes the article.

2. STATISTICAL MODELING FRAMEWORK

There are two key components in modeling the underlying storm risk of the CAT bond: the time series of storm losses at a specific location and the cross-sectional (i.e., spatial) dependence in the losses among different locations. We propose to model the former with a general 2PAR model in Section 2.1 and the latter with a semicontinuous spatiotemporal copula model in Section 2.2.

2.1. Marginal Distribution: A General 2PAR Model

Compared with other risks, storm losses have some unique characteristics. In particular, they have a large number of zero values and a continuous positive right-skewed distribution. In this article, we address these features by employing a general 2PAR model. The original 2PAR class was first introduced by Y. Wang, Yang, and Zhuang (2018) for semicontinuous time series data with excess zeros and was applied to earthquake modeling. We propose a flexible extension of Y. Wang, Yang, and Zhuang (2018) by relaxing the choice of positive continuous distributions.

Let X_{it} denote the average amount of damage to property related to storm events in location i for time period from $t-1$ to t. Also define $U_{it} = I(X_{it} > 0)$ as a Bernoulli random variable with $\mathsf{E}(U_{it}) = \rho_{it}$. We model $\{X_{it}|U_{it} = 1\}$ with a two-parameter distribution, with the distribution function F. We then model X_{it} using an F-2PAR(p, q, r) model as follows:

$$X_{it} \sim \begin{cases} F(\mu_{it}, \sigma_{it}) & \text{with probability } \rho_{it} \\ 0 & \text{with probability } (1-\rho_{it}) \end{cases}, \tag{1}$$

where autoregressive processes are further used to describe the serial correlations for each parameter, given by

$$\begin{aligned}\log(\mu_{it}) &= b_{1i} + \sum_{j=1}^{p_i} a_{1i}^{j} X_{t-j},\\ \log(\sigma_{it}) &= b_{2i} + \sum_{k=1}^{q_i} a_{2i}^{k} X_{t-k},\\ \text{logit}(\rho_{it}) &= \log\left(\frac{\rho_{it}}{1-\rho_{it}}\right) = b_{3i} + \sum_{l=1}^{r_i} a_{3i}^{l} X_{t-l}.\end{aligned}$$

Though the original Y. Wang, Yang, and Zhuang (2018) model considers lighter-tailed distributions, such as the gamma and exponential distributions, which are commonly used in the literature to model the severity of natural disasters (see, e.g., Bakshi and Madan 2002; Dassios and Jang 2003; Jaimungal and Wang 2006), many other distributions with heavier tails, such as the Lognormal (Partrat 1991; Lee and Yu 2002, 2007; Levi and Vaugirard 2003), Pareto (Burnecki, Kukla, and Weron 2000; Milidonis and Grace 2008), and Weibull (Braun 2011; Milidonis and Grace 2008) distributions, are also considered. Given the wide range of choices and mixed conclusions in the existing literature, we extend the original Y. Wang, Wang, and Zhuang (2018) model by allowing a flexible model selection for each location i from five candidate distributions: Gamma, Weibull, Lognormal, Pareto, and inverse Gaussian distributions. Furthermore, the logarithmic link function is to ensure positivity of μ_{it} and σ_{it}, and it is a common choice in the modeling of catastrophe losses (see, e.g., Y. Wang, Wang, and Zhuang 2018; Pitt et al. 2020; Li, Beirlant, and Meng 2021). The logit link is a natural choice to transform the probability of ρ_{it}.

In addition, Y. Wang, Wang, and Zhuang (2018) argued that all past events influence the current event of earthquakes and hence set $p_i = q_i = r_i = t-1$. On the other hand, Braun (2011) found that the first-order autoregressive process provided a good fit for hurricanes and earthquakes. In our empirical analysis, we propose to perform an order selection for each location based on maximum likelihood estimation (MLE). The set of parameters $\Theta_i = (b_{1i}, b_{2i}, b_{3i}, a_{1i}, a_{2i}, a_{3i}, p_i, q_i, r_i)'$ is estimated using MLE, with orders p_i, q_i, and r_i optimally determined simultaneously. Details of the probability density function, cumulative distribution function, and log-likelihood function of F-2PAR are given in Online Appendix A.

2.2. Dependence: Semicontinuous Spatiotemporal Copula Model

2.2.1. Semicontinuous Spatiotemporal Copula Model Construction

We now move on to introduce the copula construction for the storm losses among different locations. To accommodate the zero-inflation feature of storm losses, we extend the continuous spatiotemporal model in Gräler and Pebesma (2012) and Gräler (2013, 2014) using a mixed vine approach introduced by Shi and Yang (2018). Suppose $Z : \Omega \times \mathcal{S} \times \mathcal{T} \to \mathbb{R}$, where $\mathcal{S}$ is the spatial domain, $\mathcal{T}$ is the temporal domain, and Ω is the underlying probability space. Distance is the the only parameter in the formulation of bivariate spatiotemporal copula densities. Consider a random sample $\{z(s_1,t_1),...,z(s_n,t_n)\}$, where $z(s_i,t_i)$ represents the value at location s_i at time t_i for $1 \le i \le n$. When two locations are very close to each other—that is, $||s_i - s_j||$ is very small for $i \ne j$—their dependence is naturally close to perfect dependence. When two locations are separated by a very large distance—that is, $||s_i - s_j||$ is very large for $i \ne j$—then $z(s_i,t_i)$ and $z(s_j,t_j)$ tend to be independent of each other.

Pair copula construction for semicontinuous data

Adopting similar notations used in Panagiotelis et al. (2017) and Shi and Yang (2018), let Z be an element of $\boldsymbol{Z} = (Z_0, Z_1, ..., Z_d)'$ and $\boldsymbol{V}$ be a subset of $\boldsymbol{Z}$ satisfying $Z \notin \boldsymbol{V}$. Let V_h be an element of $\boldsymbol{V}$ and $\boldsymbol{V}_{\setminus h}$ be its complement. The conditional bivariate mixed distributions using a copula is given by

$$f_{Z,V_h|\boldsymbol{V}_{\setminus h}}(z,v_h|\boldsymbol{v}_{\setminus h}) = \begin{cases} C_{Z,V_h;\boldsymbol{V}_{\setminus h}}\left(F_{Z|\boldsymbol{V}_{\setminus h}}(0|\boldsymbol{v}_{\setminus h}), F_{V_h|\boldsymbol{V}_{\setminus h}}(0|\boldsymbol{v}_{\setminus h})\right) & z=0, v_h=0\\ f_{Z|\boldsymbol{V}_{\setminus h}}(z|\boldsymbol{v}_{\setminus h}) c_{1,Z,V_h;\boldsymbol{V}_{\setminus h}}\left(F_{Z|\boldsymbol{V}_{\setminus h}}(z|\boldsymbol{v}_{\setminus h}), F_{V_h|\boldsymbol{V}_{\setminus h}}(0|\boldsymbol{v}_{\setminus h})\right) & z>0, v_h=0\\ f_{V_h|\boldsymbol{V}_{\setminus h}}(v_h|\boldsymbol{v}_{\setminus h}) c_{2,Z,V_h;\boldsymbol{V}_{\setminus h}}\left(F_{Z|\boldsymbol{V}_{\setminus h}}(0|\boldsymbol{v}_{\setminus h}), F_{V_h|\boldsymbol{V}_{\setminus h}}(v_h|\boldsymbol{v}_{\setminus h})\right) & z=0, v_h>0\\ f_{Z|\boldsymbol{V}_{\setminus h}}(z|\boldsymbol{v}_{\setminus h}) f_{V_h|\boldsymbol{V}_{\setminus h}}(v_h|\boldsymbol{v}_{\setminus h}) & \\ \quad \times c_{Z,V_h;\boldsymbol{V}_{\setminus h}}\left(F_{Z|\boldsymbol{V}_{\setminus h}}(z|\boldsymbol{v}_{\setminus h}), F_{V_h|\boldsymbol{V}_{\setminus h}}(v_h|\boldsymbol{v}_{\setminus h})\right) & z>0, v_h>0 \end{cases}, \tag{2}$$

where $C_{Z,V_h;\boldsymbol{V}_{\setminus h}}(u_1,u_2)$ and $c_{Z,V_h;\boldsymbol{V}_{\setminus h}}(u_1,u_2)$ are the bivariate copula function and density function associated with $F_{Z|\boldsymbol{V}_{\setminus h}}$ and $F_{V_h|\boldsymbol{V}_{\setminus h}}$, respectively, and $c_{k,Z,V_h;\boldsymbol{V}_{\setminus h}}(u_1,u_2) = \partial C_{Z,V_h;\boldsymbol{V}_{\setminus h}}(u_1,u_2)/\partial u_k$ for $k=1$, 2. Moreover, according to Shi and Yang (2018), define

$$\tilde{f}_{Z,V_h|\boldsymbol{V}_{\setminus h}}(z,v_h|\boldsymbol{v}_{\setminus h}) := \frac{f_{Z,V_h|\boldsymbol{V}_{\setminus h}}(z,v_h|\boldsymbol{v}_{\setminus h})}{f_{Z|\boldsymbol{V}_{\setminus h}}(z|\boldsymbol{v}_{\setminus h}) f_{V_h|\boldsymbol{V}_{\setminus h}}(v_h|\boldsymbol{v}_{\setminus h})}$$
$$= \begin{cases} \dfrac{C_{Z,V_h;\boldsymbol{V}_{\setminus h}}\left(F_{Z|\boldsymbol{V}_{\setminus h}}(0|\boldsymbol{v}_{\setminus h}), F_{V_h|\boldsymbol{V}_{\setminus h}}(0|\boldsymbol{v}_{\setminus h})\right)}{F_{Z|\boldsymbol{V}_{\setminus h}}(0|\boldsymbol{v}_{\setminus h}) F_{V_h|\boldsymbol{V}_{\setminus h}}(0|\boldsymbol{v}_{\setminus h})} & z=0, v_h=0 \\ \dfrac{c_{1,Z,V_h;\boldsymbol{V}_{\setminus h}}\left(F_{Z|\boldsymbol{V}_{\setminus h}}(z|\boldsymbol{v}_{\setminus h}), F_{V_h|\boldsymbol{V}_{\setminus h}}(0|\boldsymbol{v}_{\setminus h})\right)}{F_{V_h|\boldsymbol{V}_{\setminus h}}(0|\boldsymbol{v}_{\setminus h})} & z>0, v_h=0 \\ \dfrac{c_{2,Z,V_h;\boldsymbol{V}_{\setminus h}}\left(F_{Z|\boldsymbol{V}_{\setminus h}}(0|\boldsymbol{v}_{\setminus h}), F_{V_h|\boldsymbol{V}_{\setminus h}}(v_h|\boldsymbol{v}_{\setminus h})\right)}{F_{Z|\boldsymbol{V}_{\setminus h}}(0|\boldsymbol{v}_{\setminus h})} & z=0, v_h>0 \\ c_{Z,V_h;\boldsymbol{V}_{\setminus h}}\left(F_{Z|\boldsymbol{V}_{\setminus h}}(z|\boldsymbol{v}_{\setminus h}), F_{V_h|\boldsymbol{V}_{\setminus h}}(v_h|\boldsymbol{v}_{\setminus h})\right) & z>0, v_h>0 \end{cases}. \tag{3}$$

The function $\tilde{f}_{Z,V_h;\boldsymbol{V}_{\setminus h}}$ for semicontinuous data is similar to the copula density function $c_{Z,V_h;\boldsymbol{V}_{\setminus h}}$ for the continuous case. For convenience, we will call $\tilde{f}_{Z,V_h;\boldsymbol{V}_{\setminus h}}$ a bivariate distribution function in the following discussion.

For a canonical vine, the joint distribution of $\boldsymbol{Z}$ using pair copula construction is then given by

$$f_Z(z_0, z_1, ..., z_d) = \prod_{i=0}^{d} f_{Z_i}(z_i) \prod_{i=1}^{d} \tilde{f}_{z_0,z_i}(z_0,z_i) \prod_{j=1}^{d-1} \prod_{i=1}^{d-j} \tilde{f}_{z_j,z_{j+i}|z_0,...,z_{j-1}}(z_j, z_{j+i}|z_0, ..., z_{j-1}). \tag{4}$$

Bivariate spatiotemporal distribution function

In Gräler and Pebesma (2012) and Gräler (2013, 2014), a bivariate spatial copula $c_h(u,v)$ for continuous data was formulated as a convex combination of bivariate copulas, and this dependence structure changes with distance, h. Extending this formulation to semicontinuous data, we have the bivariate spatial distribution function $\tilde{f}_h(z_i, z_{i'})$ as a convex combination bivariate distribution functions for $i \neq i'$:

$$\tilde{f}_h(z_i, z_{i'}) = \begin{cases} \tilde{f}_{1,h}(z_i, z_{i'}) & 0 \le h < l_1 \\ (1-\tau_2)\tilde{f}_{1,h}(z_i, z_{i'}) + \tau_2 \tilde{f}_{2,h}(z_i, z_{i'}) & l_1 \le h < l_2 \\ \vdots & \vdots \\ (1-\tau_k)\tilde{f}_{k-1,h}(z_i, z_{i'}) + \tau_k \cdot 1 & l_{k-1} \le h < l_k \\ 1 & l_k \le h \end{cases}, \tag{5}$$

where h is the separating distance between the pair of locations, k is the chosen number of distance bins, $l_1, ..., l_k$ denote the value of each of the k distances, and $\tau_j = \frac{h-l_{j-1}}{l_j - l_{j-1}}$ are weights associated with bivariate distribution function $\tilde{f}_{j,h}(z_i, z_{i'})$. τ_js are linearly interpolated based on the separating distance h and distances l_{j-1} and l_j. Moreover, each bivariate distribution function in Equation (5) depends on the separating distance only and is estimated independently. This ensures the smoothness of the bivariate spatial copula function, which is fully parameterized by distance. When two locations have a very large separating distance—that is, $h \ge l_k$—z_i and $z_{i'}$ are independent and $\tilde{f}_h(z_i, z_{i'}) = 1$.

Further extending from the bivariate spatial distribution functions, the bivariate spatiotemporal distribution function, $\tilde{f}^{\Delta}_h(z_i, z_{i'})$, is another convex combination of bivariate distribution functions at different time lags Δ. For a pair of locations with a separating distance $l_{j-1} \le h < l_j$ and time lag Δ, the bivariate spatiotemporal distribution function is given by

$$\tilde{f}^{\Delta}_h(z_i, z_{i'}) = (1-\tau_j)\tilde{f}^{\Delta}_{j-1,h}(z_i, z_{i'}) + \tau_j \tilde{f}^{\Delta}_{j,h}(z_i, z_{i'}). \tag{6}$$

Spatiotemporal vine structure

To complete the spatiotemporal copula construction, a vine copula structure is employed to join the previously formulated spatiotemporal bivariate copulas into multivariate copulas (Bedford and Cooke 2002; Aas et al. 2009; Gräler and Pebesma 2012; Gräler 2013, 2014). We use canonical vines here because all initial dependencies are with respect to the central location. With a value at the central location and d values in the spatiotemporal neighborhood, a $d+1$-dimensional vine copula is constructed. The overall structure of the first spatiotemporal vine copula tree is shown in Figure 1. Each edge represents a

bivariate spatiotemporal distribution function formulated in Equation (6). The remaining bivariate distribution functions in the upper trees are estimated such that they employ fixed copula families with fixed parameters regardless of where the central location is and how the neighborhood is spatiotemporally organized. Figure 2 shows an example of upper trees of a 10-dimensional vine copula. Each edge represents a fixed bivariate distribution function.

Combining the marginal densities and spatiotemporal and fixed bivariate distribution functions, the joint probability density function is the product of the three components, shown in Equation (7) below:

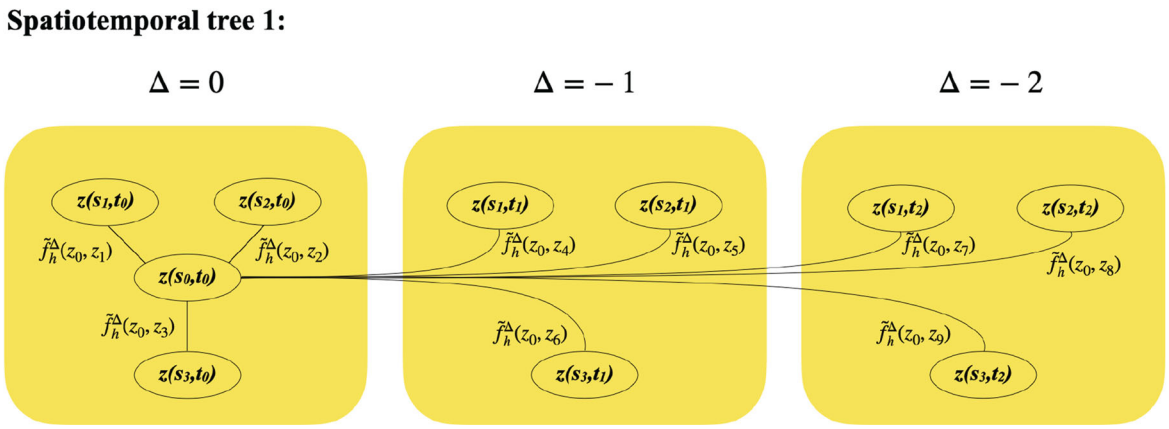


FIGURE 1. Tree 1 of a 10-Dimensional Vine Copula.

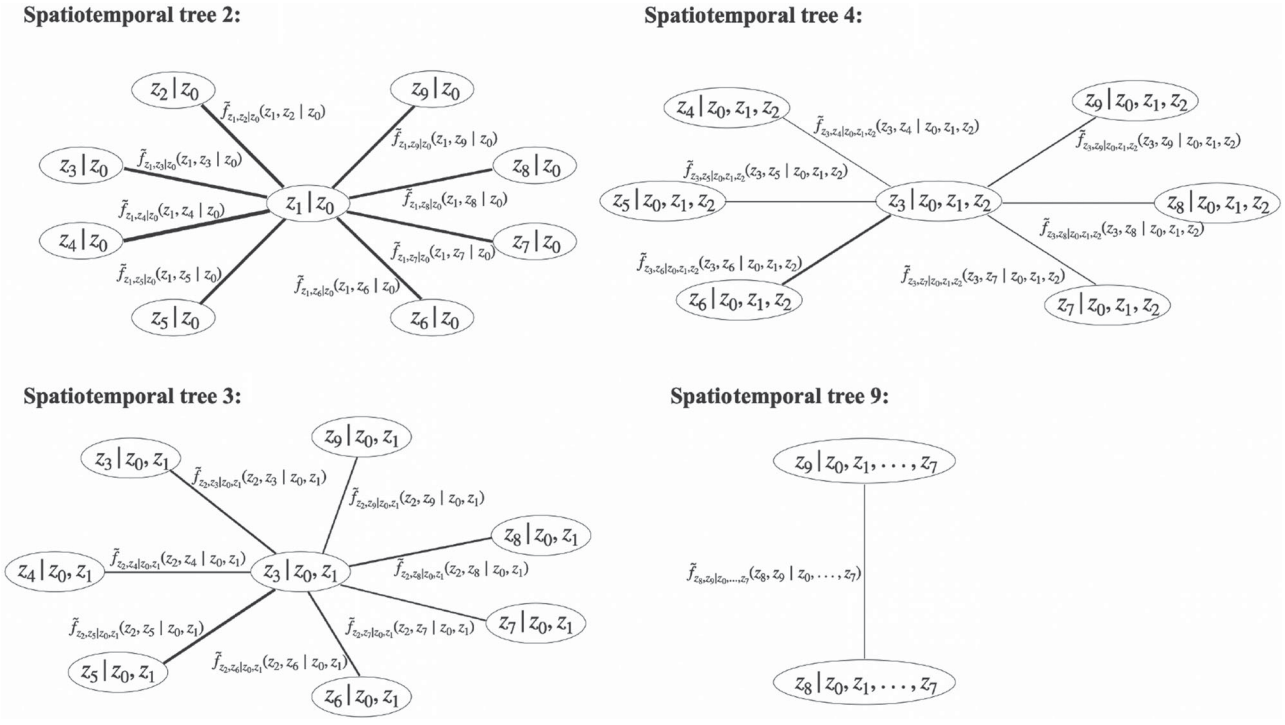


FIGURE 2. Representative Upper Trees of a 10-Dimensional Vine Copula.

$$f_Z(z_0, z_1, ..., z_d) = \prod_{i=0}^{d} f_{Z_i}(z_i) \prod_{i=1}^{d} \tilde{f}_h^{\Delta}(z_0, z_i) \prod_{j=1}^{d-1} \prod_{i=1}^{d-j} \tilde{f}_{z_j, z_{j+i}|z_0, ..., z_{j-1}}(z_j, z_{j+i}|z_0, ..., z_{j-1}). \quad (7)$$

2.2.2. Estimation Procedure

The general estimation procedure for spatiotemporal copula vine trees is summarized in Figure 3 and Algorithm 1. The first spatiotemporal vine tree, which consists of spatiotemporal bivariate copulas shown in Figure 1, is first estimated using Steps 1 to 5 in Algorithm 1. A copula's Kendall's tau value relies on the double integral of the copula and, thus, there is a one-to-one relationship between Kendall's tau and their parameter in some one-parameter copula families (Nelsen 2007). In Step 4, several copula families are fitted to the data and the copula model with the best fit is selected. We choose among Gaussian, Student's *t*, Clayton, Gumbel, and Frank copulas. These families exhibit a direct link between Kendall's tau and their parameters. A convex combination of two bivariate copulas results in a convex combination of two Kendall's tau values with a given separating distance *h*. In this estimation procedure, the separating distance between two locations *h*, which is the only parameter of the bivariate copulas, determines Kendall's tau value and thus directly corresponds to the copula parameters. This guarantees the smoothness of the copula function with distance.

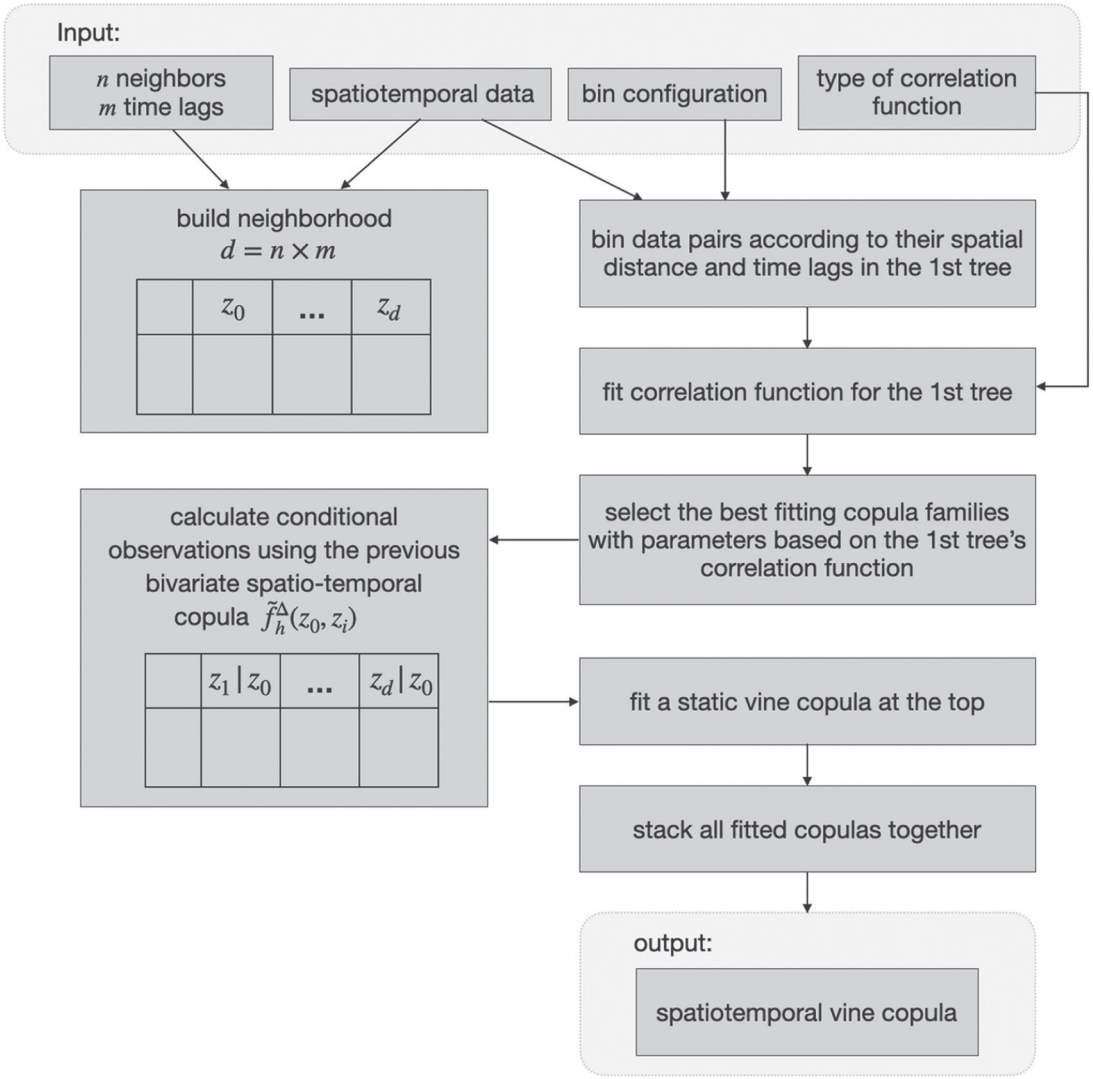


FIGURE 3. Flowchart of the Estimation Procedure.

The upper vine structure is spatiotemporally fixed, as shown in the example in Figure 2. It is estimated using Steps 6 to 7 in Algorithm 1. The same upper vine structure with the same copula families and parameters is used for every spatiotemporal vine structure around each central location.

Algorithm 1: Spatiotemporal copula estimation

Estimation of the first spatio-temporal vine tree

Result: bivariate spatio-temporal distribution functions in the first spatio-temporal vine tree

for *each time lag* Δ **do**

Step 1 All spatial data at different time lags are grouped into k distance bins pairwise according to their spatial separation distance.

Step 2 Kendall's tau correlation is calculated for each of the k separation distances and an empirical correlogram is calculated using Kendall's tau.

Step 3 Fit a polynomial function to the empirical correlogram obtained in the previous step.

Step 4 For each distance bin, several copula families are fitted to the data and the family with the best fit (highest log-likelihood) is selected.

Step 5 The bivariate distribution functions are obtained using Equation (6).

end

Estimation of the spatio-temporally fixed upper vine

Result: bivariate copulas in the upper vine

Step 6 The data are grouped in spatio-temporal neighborhoods of central locations and their spatially closest n neighbors at m time lags. The spatio-temporal tree is $(d+1)$-dimensional with $d = n \times m$.

Step 7 The bivariate spatio-temporal distribution functions $\tilde{f}_h^{\Delta}(z_0, z_i)$ on the first tree are now used to derive the conditional sample of dimension d (conditioned to the value at the central location) to fit the remainder of the spatio-temporal canonical vine, which is spatio-temporally fixed. The vine copula estimation proceeds sequentially by using the best fitting copula per bivariate pair.

3. STORM CAT BOND

In this section, we discuss the storm CAT bond market, the proposed storm CAT bond structure, as well as the pricing framework. In this article, we focus on storm risk management, but the bond design and pricing framework are generally applicable to other catastrophe risks as well. For ease of reference, the definitions of key variables to be used in this section are provided in Table 1.

3.1. The Storm CAT Bond Market

Figure 4 shows the transactions between insurers, reinsurers, and investors. At the start of each year, an insurer i buys an excess of loss (XL) cover from the reinsurer with a premium of $\pi_{i,t-1}$ to reduce its exposure to extreme storm losses. At the end of each year, the reinsurer has a benefit payable of $B_{i,t}$ to insurer i. To transfer the risk of storm CAT losses to an investor, the reinsurer issues an n-year storm CAT bond whose structure will be discussed in Section 3.2. The bond issuer can be any reinsurance company with storm CAT liabilities and wishes to transfer risks to the capital market. The bond investor can be

TABLE 1
Definitions of Variables

Variable	Definition
$\alpha_{i,t}$	Quantity of the reinsurance policy purchased by insurer i from $t-1$ to t
$D_{i,t}$	Deductible of the reinsurance policy purchased by insurer i from $t-1$ to t
$M_{i,t}$	Limit of the reinsurance policy purchased by insurer i from $t-1$ to t
$L_{i,t}$	Average losses per event experienced by insurer i from $t-1$ to t
$B_{i,t}$	Benefit payout to insurer i from $t-1$ to t $B_{i,t} = \alpha_{i,t}\min(\max(L_{i,t} - D_{i,t}, 0), M_{i,t})$
B_t	Total benefit payout to all buyers of the reinsurance policy at time t $B_t = \sum_{i=1}^{\ell} B_{i,t}$ with a total of ℓ buyers
k	A simple loading applied on the total expected benefit payout
$\pi_{i,t-1}$	Total reinsurance premium received from insurer i at time $t-1$ $\pi_{i,t-1} = (1+k) \times \mathsf{E}^{\mathbb{P}}[B_{i,t}]$
π_{t-1}	Total reinsurance premium received from all buyers of the reinsurance policy at time $t-1$ $\pi_{t-1} = (1+k) \times \mathsf{E}^{\mathbb{P}}[B_t] = \sum_{i=1}^{\ell} \pi_{i,t-1}$
η_t	Catastrophe index at time t Defined as the sum of average losses per event at time t: $\eta_t = \sum_{i=1}^{\ell} L_{i,t}$ with a total of ℓ buyers
P	Price/premium of the CAT bond
n	Term to maturity of the CAT bond
δ_1, δ_2	First and second trigger level in the CAT bond
c_1, c_2	$\delta_1 + c_1$ and $\delta_2 + c_2$ are the triggers beyond which coupon and principal payouts reduce to zero in the partial reduction design, respectively
CP	Maximum coupon payout of the CAT bond for period t
$C_{cat,t}$	Actual coupon payout of the CAT bond for period t
FV	Face value/maximum principal payout of the CAT bond upon maturity
R_{cat}	Actual principal payout of the CAT bond upon maturity
w^R	Initial wealth of the reinsurer
w^I	Initial wealth of the investor
C_{rf}	Coupon payout of a risk-free bond
R_{rf}	Principal payout of a risk-free bond
S_t	Value of stock held by the investor at time t
r_f	Risk-free rate

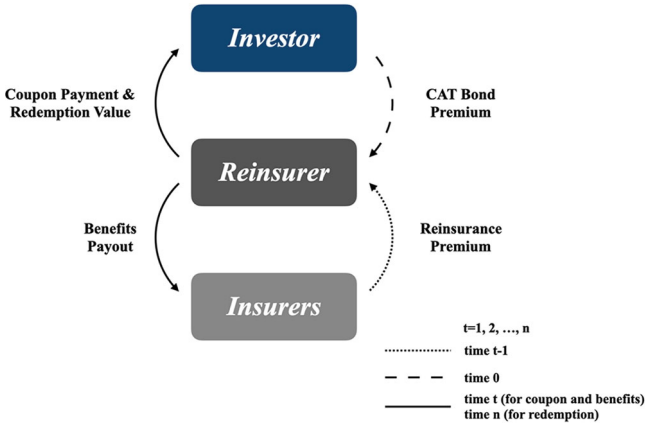


FIGURE 4. Flowchart of the CAT Bond Market.

any individual or institutional investor who wishes to earn potentially high returns from the CAT bond or to diversify its investment portfolio.[3]

3.2. The Storm CAT Bond Structure

The bond issuer collects a premium up front and pays coupons and principal to the investor. Suppose the bond is designed to mature at the end of year n. An investor first pays a fixed bond premium P at the inception of the bond. In return, the bond issuer pays the investor annual coupons at the end of each year and the principal value upon maturity of the bond. Because CAT bonds are highly customizable and multiple triggers can be used to tailor the risks (Braun and Kousky 2021), we propose a double-trigger bond payment structure with the coupons and principal amount both dependent on η_t, a catastrophe index at time t. We will consider both a binary reduction and a partial reduction design, outlined below.

Binary Reduction Design In a binary reduction design, the coupon or principal payout is immediately reduced to zero once the trigger is reached. In particular, if η_t stays below the first trigger level δ_1, the maximum coupon amount CP is paid to the investor at time t. On the other hand, when η_t exceeds δ_1, the coupon payout at time t is reduced to zero. Moreover, if η_t, at any time during the n years, exceeds the second trigger level δ_2 ($\delta_2 > \delta_1$), all future payouts, including future coupons and the principal payout upon maturity, will be reduced to zero. Otherwise, the full amount FV is paid to the investor upon maturity. Denote $\eta^{\max} = \max_{1\le t\le n}\{\eta_t\}$ as the maximum catastrophe index over the bond's n-year term and $\eta_t^{\max} = \max_{1\le s\le t-1}\{\eta_s\}$ as the maximum catastrophe index over periods up to time $t-1$. In summary, the coupon payout at time t, $C_{cat,t}$, and the principal payout upon maturity, R_{cat}, are given respectively by

$$C_{cat,t}(\eta_t, \eta_t^{\max}) = \begin{cases} 0 & \text{if } \eta_t^{\max} \ge \delta_2 \text{ or } \eta_t \ge \delta_1 \\ CP & \text{if } \eta_t^{\max} < \delta_2 \text{ and } \eta_t < \delta_1 \end{cases} \tag{8}$$

and

$$R_{cat}(\eta^{\max}) = \begin{cases} 0 & \text{if } \eta^{\max} \ge \delta_2 \\ FV & \text{if } \eta^{\max} < \delta_2 \end{cases}. \tag{9}$$

Partial Reduction Design In addition to the binary reduction design, we consider a partial reduction design for both coupon and principal payouts. Let δ_1 and δ_2 be the trigger levels defined in Table 1, above which the coupon or the principal payout will be reduced to zero linearly, respectively. Further define $\delta_1 + c_1$ as the trigger level that the coupon payout is reduced to zero and $\delta_2 + c_2$ as the trigger level that the principal payout is reduced to zero. Mathematically, the coupon payout in period t is

$$C_{cat,t}(\eta_t, \eta_t^{\max}) = \begin{cases} 0 & \text{if } \eta_t^{\max} \ge \delta_2 \text{ or } \eta_t \ge \delta_1 + c_1 \\ \dfrac{CP}{c_1}(\delta_1 + c_1 - \eta_t) & \text{if } \eta_t^{\max} < \delta_2 \text{ and } \delta_1 \le \eta_t < \delta_1 + c_1 \\ CP & \text{if } \eta_t^{\max} < \delta_2 \text{ and } \eta_t < \delta_1 \end{cases}, \tag{10}$$

where we assume $\delta_1 + c_1 \le \delta_2$. The principal payout upon maturity is

$$R_{cat}(\eta^{\max}) = \begin{cases} 0 & \text{if } \eta^{\max} \ge \delta_2 + c_2 \\ \dfrac{FV}{c_2}(\delta_2 + c_2 - \eta^{\max}) & \text{if } \delta_2 \le \eta^{\max} < \delta_2 + c_2 \\ FV & \text{if } \eta^{\max} < \delta_2 \end{cases}. \tag{11}$$

[3]Typically, CAT bond issuance is achieved through a special purpose vehicle (SPV). For example, the reinsurer could purchase a reinsurance contract from an SPV, and the SPV would issue CAT bonds to different tranches of investors. SPV could pool assets from different operating entities and, more important, reduce issuer default risk. In this article, we ignore default risk for simplicity of the analysis and assume that reinsurers issue CAT bonds directly to investors.

3.3. The Storm CAT Bond Valuation

3.3.1. Wang Transform for Bond Price

The pricing methodology employed in this article uses the equivalent martingale measure identified by Wang transform (S. S. Wang, 1996, 2000, 2002), which has been widely applied in securities pricing in incomplete markets (see, e.g., Lin and Cox 2005; Dowd et al. 2006; Denuit, Devolder, and Goderniaux 2007; Galeotti, Gürtler, and Winkelvos 2013).[4] More specifically, the bond price, P, can be computed based on the expected discounted coupons and principal payouts under an equivalent martingale measure $\mathbb{Q}$:

$$P = \mathsf{E}^{\mathbb{Q}}[R_{cat}]d(0,n) + \sum_{t=1}^{n} \mathsf{E}^{\mathbb{Q}}[C_{cat,t}]d(0,t), \tag{12}$$

where $d(0,t) \in (0,1)$ is the discount factor for cash flow at time t.

We employ Wang's distortion risk measure to convert distribution functions between the real-world probability measure $\mathbb{P}$ and a risk-neutral probability measure $\mathbb{Q}$. In particular, the distorted (a.k.a. risk-adjusted) distribution, $F_t^{\mathbb{Q}}(u)$, for a given distribution $F_t(u)$ is defined by

$$F^{\mathbb{Q}}(u) = \Phi\left[\Phi^{-1}(F(u)) - \lambda\right], \tag{13}$$

where λ is a parameter representing the market price of risk. More specifically, the distorted distribution for the principal payout is

$$F^{\mathbb{Q}}_{\eta^{\max}}(u) = \Phi\left[\Phi^{-1}(\mathbb{P}(\eta^{\max} \le u)) - \lambda\right], \tag{14}$$

and the distorted distribution for the coupon payout at time t is

$$F^{\mathbb{Q}}_{\eta_t,\eta_t^{\max}}(u_1,u_2) = \Phi\left[\Phi^{-1}\left(\mathbb{P}\left(\eta_t \le u_1, \eta_t^{\max} \le u_2\right)\right) - \lambda\right]. \tag{15}$$

The detailed pricing formula is provided in Online Appendix B. When the CAT bond is sold at par—that is, $P = FV$—the maximum coupon rate, CP/FV, increases monotonically with an increasing value of the risk premium, λ.

3.3.2. Determining Equilibrium Market Price of Risk and Issue Size

In the above equivalent martingale pricing framework, the most critical issue is to determine the appropriate market price of risk, λ, and hence the equilibrium issue size. This is particularly challenging in an embryonic market where very limited storm CAT bonds are traded. In this article, we endogenously determine the equilibrium market price of risk and the issue size based on market supply and demand. The corresponding numerical analysis will be discussed in Section 5.2.

Supply side from the reinsurer's perspective We first determine the quantity of the CAT bond that the reinsurer is willing to sell by considering the reinsurer's portfolio and risk preferences only. Starting with an initial wealth of w^R, the reinsurer collects insurance premiums, a total of π_{t-1}, from insurers at the beginning of each year and pays insurance benefits, a total of B_t, to insurers at the end of each year. The reinsurance policy is assumed to be an XL cover with a deductible of $D_{i,t}$ and a limit of $M_{i,t}$ for insurer i for time period $t-1$ to t. π_{t-1} is calculated by adding a loading k to the expectation of B_t; that is, $\pi_{t-1} = (1+k) \times \mathsf{E}^{\mathbb{P}}[B_t]$. Moreover, the reinsurer issues a storm CAT bond to an investor and pays out coupons and principal values, which are contingent on the severity of storms (see Eqs. [8] to [11]). The reinsurer's wealth at the end of each year is

[4]For example, Galeotti, Gürtler, and Winkelvos (2013) compared different premium calculation models and found that theWang transform has consistently accurate predictive power.

$$\begin{aligned} W_0^R &= w^R + \pi_0 + \theta^r P, \\ W_1^R &= W_0^R(1+r_f) + \pi_1 - B_1 - \theta^R C_{cat,1}, \\ W_2^R &= W_1^R(1+r_f) + \pi_2 - B_2 - \theta^R C_{cat,2}, \\ &\vdots \\ W_n^R &= W_{n-1}^R(1+r_f) - B_n - \theta^r C_{cat,n} - \theta^R R_{cat}. \end{aligned} \tag{16}$$

The quantity θ^R represents the issue size of the bond, which is determined by the reinsurer. The optimal quantity θ^R is calculated by maximizing the mean–variance objective of the reinsurer's wealth at the end of year n; that is,

$$\theta^R = \operatorname{argmax}_{\theta^r \in \mathbb{R}_+} \left[\mathsf{E}\left(W_n^R\right) - \gamma^R \mathsf{Var}\left(W_n^R\right) \right], \tag{17}$$

where γ^R is a parameter that indicates the reinsurer's level of risk aversion. In the rest of the article we will use $\mathsf{E}[\cdot], \mathsf{Var}[\cdot]$, and $\mathsf{Cov}[\cdot]$ to denote $\mathsf{E}^{\mathbb{P}}[\cdot], \mathsf{Var}^{\mathbb{P}}[\cdot]$, and $\mathsf{Cov}^{\mathbb{P}}[\cdot]$, respectively, when it does not cause ambiguity. By solving Equation (17), we obtain the optimal issue size for the reinsurer. This result is summarized in Proposition 1.

Proposition 1. *The maximizer to Problem (17) is uniquely given by*

$$\theta^R = \max\left\{ \frac{N^R}{DN^R}, 0 \right\}, \tag{18}$$

where

$$N^R = P(1+r_f)^n - E\left[\sum_{t=1}^{n} C_{cat,t}(1+r_f)^{n-t} \right] - E[R_{cat}]$$

$$-2\gamma^R \left\{ \mathsf{Cov}\left(\sum_{t=1}^{n} B_t(1+r_f)^{n-t}, \sum_{t=1}^{n} C_{cat,t}(1+r_f)^{n-t} \right) + \mathsf{Cov}\left(\sum_{t=1}^{n} B_t(1+r_f)^{n-t}, R_{cat} \right) \right\},$$

and

$$DN^R = 2\gamma^R \left\{ \mathsf{Var}\left(\sum_{t=1}^{n} C_{cat,t}(1+r_f)^{n-t} \right) + \mathsf{Var}(R_{cat}) + 2\mathsf{Cov}\left(\sum_{t=1}^{n} C_{cat,t}(1+r_f)^{n-t}, R_{cat} \right) \right\}.$$

Proof. See Online Appendix C.1. □

Because the bond is sold at par, at a given λ value, the maximum coupon rate CP/FV can be solved using Equation (12) by setting $P = FV$. The optimal quantity, θ^R, then depends on the maximum coupon rate CP/FV and hence the value of λ.

Demand side from the investor's perspective Likewise, we now determine the quantity of the CAT bond that the investor is willing to buy by considering the investor's portfolio and risk preferences. Let us assume that the investor's initial portfolio includes an n-year risk-free bond with a face value of R_{rf}, which is bought at par, and a stock portfolio with a value of S_t at time t. Without loss of generality, we assume that the investor's stock portfolio tracks the market portfolio and follows the S&P500 market rate with a Lognormal distribution. The investor also buys θ^i units of storm CAT bond from the reinsurer. Excluding the initial stock value S_0, the investor starts with an initial wealth w^I. The investor's wealth at the end of each year is then given in Equation (19):

$$\begin{aligned} W_0^I &= w^I - R_{rf} + S_0 - \theta^i P^I, \\ W_1^I &= (W_0^I - S_0)(1 + r_f) + C_{rf} + S_1 + \theta^i C_{cat,1}, \\ &\vdots \\ W_n^I &= (W_{n-1}^I - S_{n-1})(1 + r_f) + C_{rf} + S_n + R_{rf} + \theta^i C_{cat,n} + \theta^i R_{cat}, \end{aligned} \tag{19}$$

where $C_{rf} = r_f R_{rf}$.

The optimal CAT bond quantity the investor is willing to buy, θ^I, is then calculated by maximizing the investor's mean–variance objective of its wealth at the end of year n; that is,

$$\theta^I = \arg\max_{\theta^i \in \mathbb{R}_+} \left[\mathsf{E}\left(W_n^I\right) - \gamma^I \mathsf{Var}\left(W_n^I\right)\right]. \tag{20}$$

where γ^I is a parameter that indicates the investor's level of risk aversion. We assume that the storm CAT bond is uncorrelated with the stock market.[5] The optimal amount of CAT bonds the investor would like to buy is given in Proposition 2.

Proposition 2. *The maximizer to Problem (20) is uniquely given by*

$$\theta^I = \max\left\{\frac{N^I}{DN^I}, 0\right\}, \tag{21}$$

where

$$N^I = -P(1 + r_f)^n + \mathsf{E}\left[\sum_{t=1}^{n} C_{cat,t}(1 + r_f)^{n-t}\right] + \mathsf{E}[R_{cat}]$$

and

$$DN^I = 2\gamma^I \left\{\mathsf{Var}\left(\sum_{t=1}^{n} C_{cat,t}(1 + r_f)^{n-t}\right) + \mathsf{Var}(R_{cat}) + 2\mathsf{Cov}\left(\sum_{t=1}^{n} C_{cat,t}(1 + r_f)^{n-t}, R_{cat}\right)\right\}.$$

Proof. See Online Appendix C.2. □

In particular, θ^I, depends on the maximum coupon rate *CP*/*FV* and hence the value of λ.

Once we obtain both the supply and demand functions, we may determine the equilibrium market price of risk and the issue size endogenously by considering both the reinsurer's and a representative investor's risk preferences. To obtain the equilibrium issue size, we equate θ^R in Equation (18) and θ^I in Equation (21); that is, $\theta^R = \theta^I$. This way, we can solve for the maximum coupon rate *CP*/*FV* at the equilibrium quantity. Numerical analysis details are investigated in Section 5.2.

4. EMPIRICAL ESTIMATION RESULTS

4.1. Data

In the empirical analysis, we use data obtained from the Storm Events Database[6] maintained by the National Oceanic and Atmosphere Administration. We compile the annual property losses due to storm events (storm losses) in each of the 67 counties in Florida from 1950 to 2019. We model the longitudinal annual storm losses in each county in Florida from 1950 to 2019 using the marginal distribution discussed in Section 2.1 and the dependence model discussed in Section 2.2.

Table 2 summarizes the key statistics of the storm losses at the state level, including the mean, standard deviation, skewness, median, 95% Value at Risk (VaR), and 99% VaR of average loss and frequency. Average loss (in million dollars) refers to the average annual property losses per storm event after inflation adjustment. Frequency refers to the number of storm

[5]Although there is some evidence that suggests some correlation between corporate bond prices and CAT bond prices (Gürtler, Hibbeln, and Winkelvos 2016), it is generally believed that the CAT bond and financial markets are uncorrelated (Froot et al. 1995; Canter, Cole, and Sandor 1996; Bantwal and Kunreuther 2000; Karagiannis et al. 2016; Tang and Yuan 2019).

[6]Available at https://www.ncdc.noaa.gov/stormevents/.

TABLE 2
Florida State-Level Summary Statistics

No. of counties	67	
No. of years	70 (1950–2019)	
	Average loss (in million dollars)	Frequency (no. of events)
Mean	468.37	340.26
SD	1900.50	338.88
Skewness	6.16	0.93
Median	27.81	173.00
95% VaR	2334.96	995.95
99% VaR	8202.92	1072.64

Note: Average loss refers to the average annual property loss per storm event after adjusting for inflation. Frequency refers to the number of storm events every year. The product of average loss and frequency is the annual aggregated property losses due to storm events in that year.

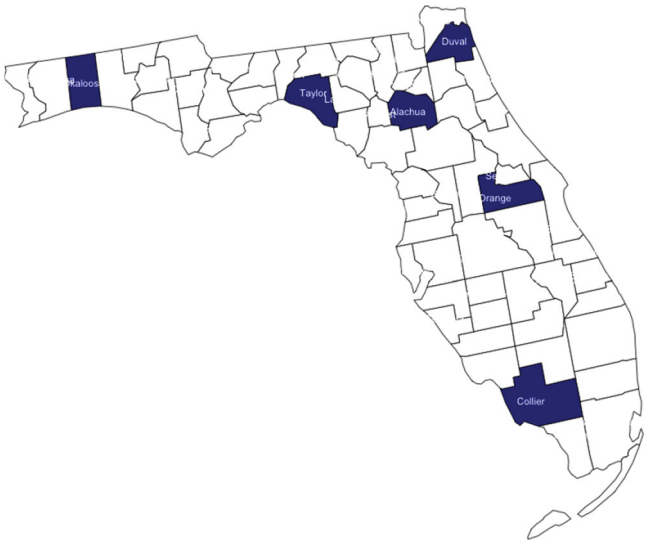


FIGURE 5. Locations of the Representative Counties.

events every year. The product of average loss and frequency is the annual aggregated property losses due to storm events in that year.

We illustrate county-level information by showing six representative counties in the dataset. Figure 5 shows the locations of the six representative counties in Florida. Table 3 summarizes the information and key statistics of average loss in six representative counties in Florida. Figure 6 plots the time series of the average losses (in million dollars) in the six representative counties from 1950 to 2019. We can observe from the plots that the longitudinal data in all counties have a large number of zero values with a handful of spikes. These characteristics led to our choice of the Dist-2PAR model discussed in Section 2.1 as the marginal model.

4.2. Marginal Distribution Estimation Results

The estimates of parameters $\hat{\Theta}_i = (\hat{b}_{1i}, \hat{b}_{2i}, \hat{b}_{3i}, \hat{a}_{1i}, \hat{a}_{2i}, \hat{a}_{3i}, \widehat{p_i}, \widehat{q_i}, \widehat{r_i})'$ formulated in Equation (1) for each county i are obtained using MLE (details in Online Appendix A), with $\hat{a}_{1i}, \hat{a}_{2i}, \hat{a}_{3i}$ restricted to values between 0 and 1. The distribution with the highest likelihood is selected for each location i (see details in Online Appendix D). By the invariance property of MLE, estimates of $\hat{\mu}_{it}$ and $\hat{\rho}_{it}$ are obtained from the estimated parameters, $\hat{\Theta}_i$:

TABLE 3
Summary Statistics of Representative Counties in Florida

County Name	Alachua	Collier	Duval	Okaloosa	Orange	Taylor
Longitude	–82.36	–81.35	–81.67	–86.59	–81.32	–83.60
Latitude	29.67	26.11	30.33	30.69	28.51	30.05
Average loss (in million dollars)						
Mean	0.38	0.27	0.34	1.41	1.46	0.24
SD	1.33	0.78	0.94	4.49	4.59	0.76
Skewness	4.89	3.99	3.86	4.11	4.26	4.72
Median	0.00	0.00	0.02	0.06	0.03	0.00
95% VaR	2.25	0.85	1.92	6.87	7.62	1.55
99% VaR	6.00	3.86	4.97	22.26	22.17	3.26

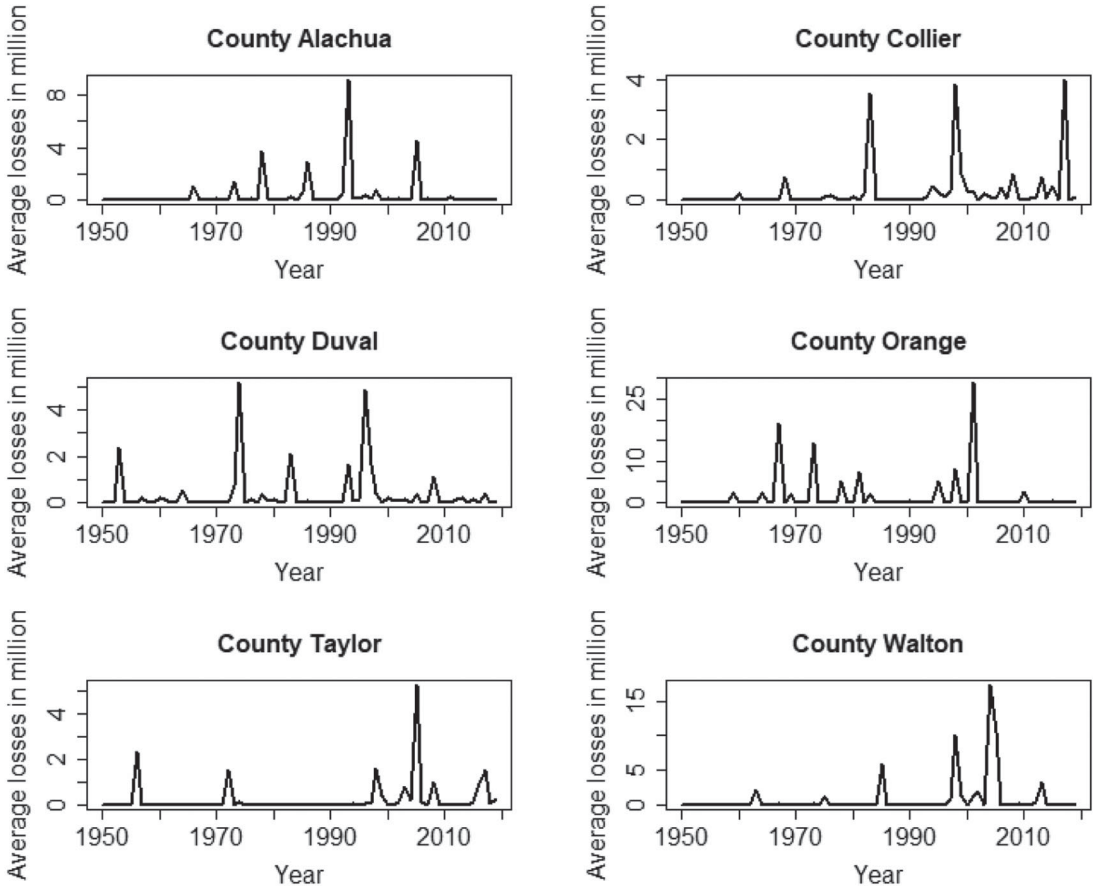


FIGURE 6. Average Losses (in Million Dollars) of Representative Counties from 1950 to 2019.

$$\begin{aligned} \hat{\mu}_{it} &= \exp\left(\hat{b}_{1i} + \sum_{j=1}^{t-1} \hat{a}_{1i}^{j} X_{t-j}\right), \\ \hat{\rho}_{it} &= \frac{1}{1 + \exp\left(-\hat{b}_{3i} - \sum_{l=1}^{t-1} \hat{a}_{3i}^{l} X_{t-l}\right)}. \end{aligned} \tag{22}$$

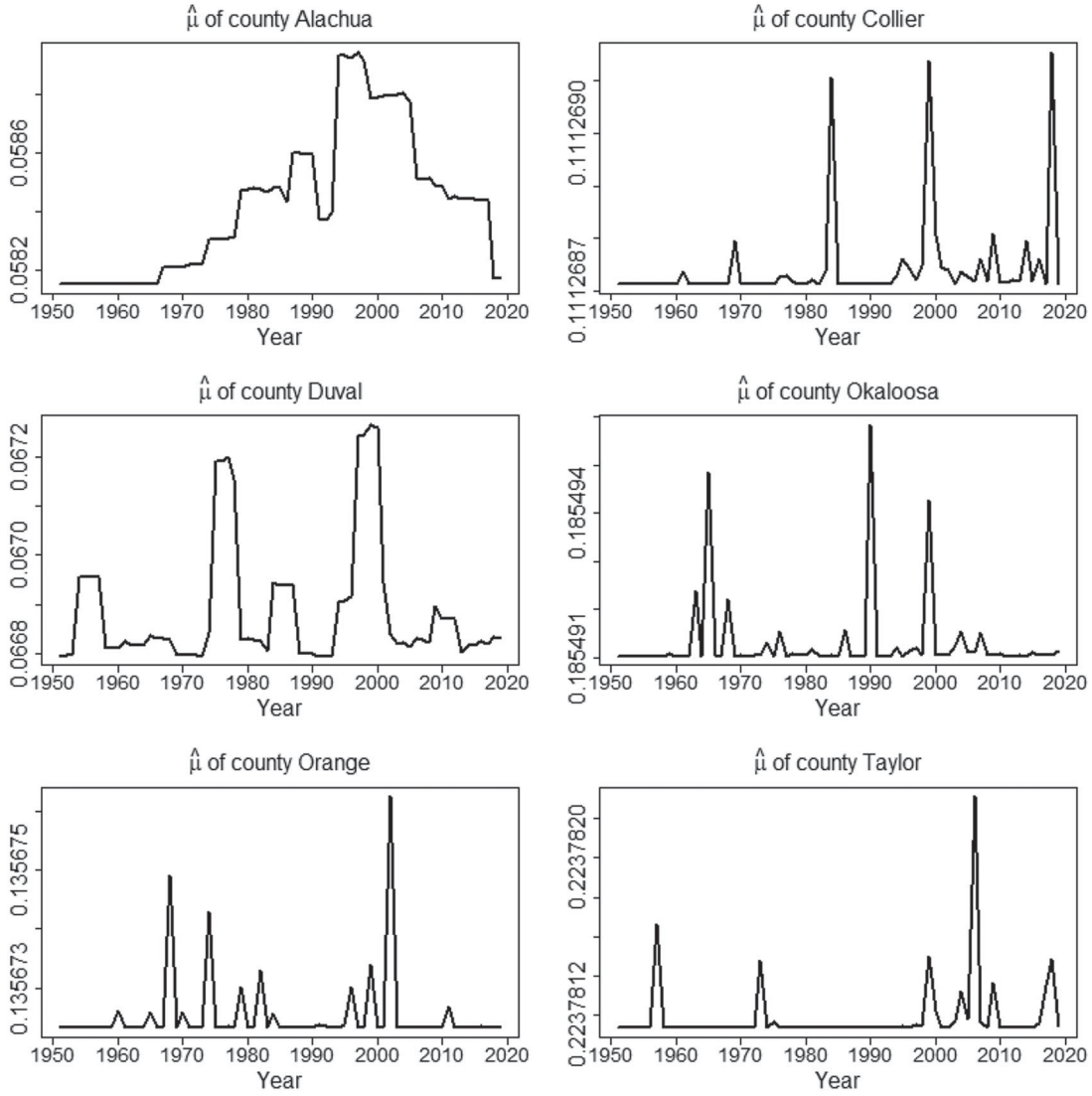


FIGURE 7. μ_{it} Plot of Representative Counties.

Figure 7 and Figure 8 show plots of the estimated $\hat{\mu}_{it}$ and $\hat{\rho}_{it}$, respectively, in the six representative counties from 1951 to 2019. We observe from Figure 7 that $\hat{\mu}_{it}$ has a similar pattern with the time series of storm losses in Figure 6: there are a few spikes in values, though most values stay close to the minimum. This is because large values of X_{it} have immediate impact on subsequent values of $\hat{\mu}_{it}$, as seen from Equation (22). The impact of a large X_{it} fades over time owing to the increasing power in $\hat{\alpha}_{1i}^{j}$.

Inspecting the time series of $\hat{\rho}_{it}$, the estimated probability of having positive storm losses in a given year, in Figure 8 we see a general increasing trend over time. This is consistent with the storm data observed, which exhibit an increasing frequency of storm events over the years. This is also consistent with research findings in the literature (see, e.g., Dunstone et al. 2013; Myhre et al. 2019; Murakami et al. 2020), which present evidence of increasing frequency of storm events. Some additional diagnostic tests illustrated by ACF and PACF for the representative counties are provided in Online Appendix E.

4.3. Spatiotemporal Copula Estimation Results

Each of the bivariate copulas shown in Figures 1 and 2 is estimated using the estimation procedure discussed in Section 2.2.2. When estimating spatiotemporal bivariate copulas in the first tree of the vine, we select from Gaussian, Clayton, Gumbel, Student's t, and Frank copulas whose parameters exhibit a direct link with Kendall's tau. Detailed estimation results

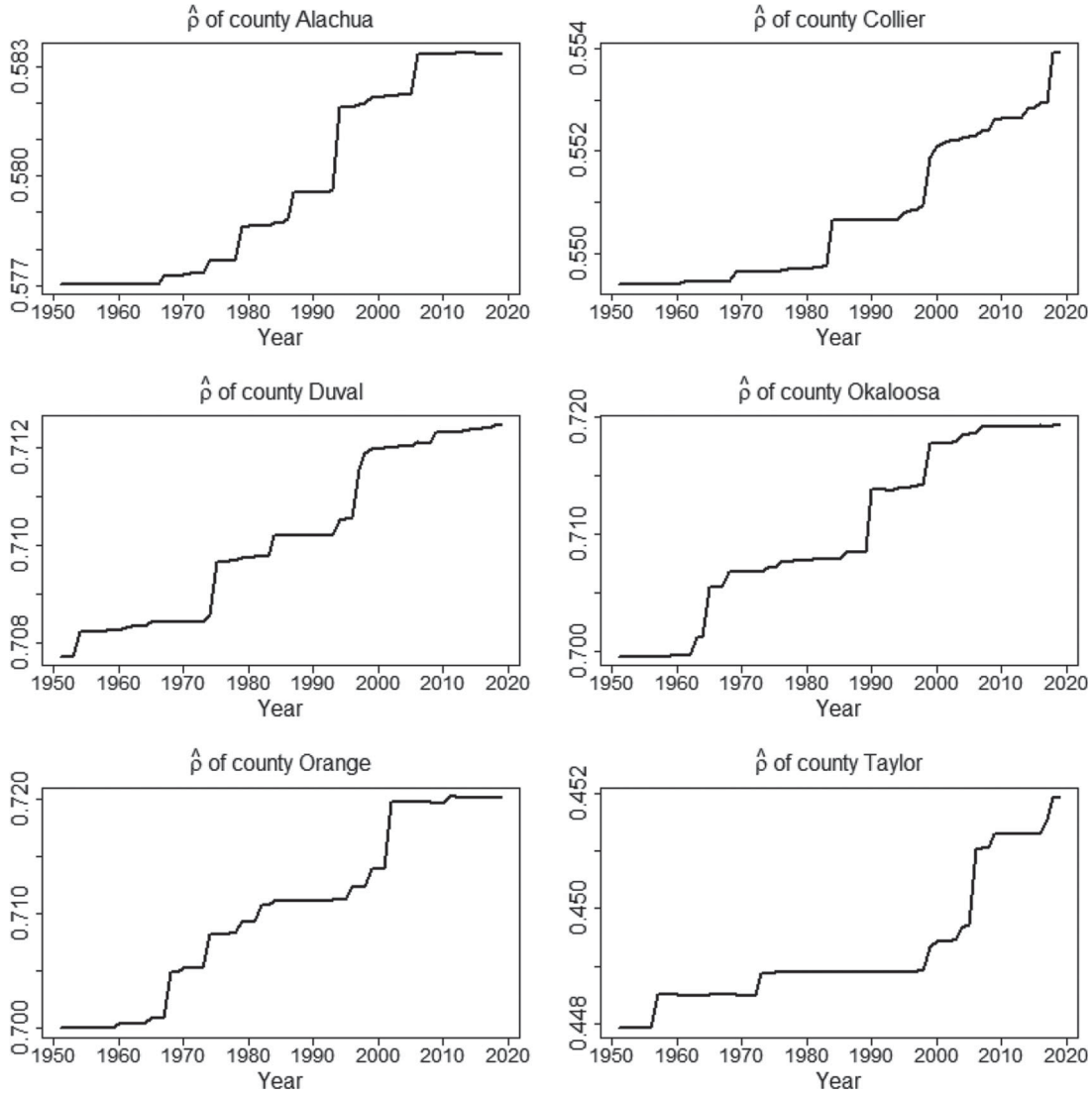


FIGURE 8. ρ_{it} Plot of Representative Counties.

are provided in Online Appendix F. The thicknesses of the edges shown in Figure 2 are proportional to the estimated Kendall's tau values in the spatiotemporally fixed upper vine trees.

5. STORM CAT BOND VALUATION RESULTS

Previously, we successfully applied the 2PAR spatiotemporal copula framework to modeling storm losses. In this section, we apply the estimation results to storm CAT bond design and valuation. We will introduce bond parameters in Section 5.1. Then we will discuss bond valuation in equilibrium market price of risk in Section 5.2.

5.1. Bond Parameters

To build the reinsurer's and the investor's asset portfolios in Equations (16) and (19), we make the following assumptions:

- Insurers in the same county are collectively treated as one insurer. Thus, there are a total of 67 insurers in Florida.
- Each insurer purchases the XL cover with one unit quantity; that is, $\alpha_{i,t} = 1$. Thus, we have the total reinsurance benefit payout $B_t = \sum_{i=1}^{67} \min(\max(L_{i,t} - D_{i,t}, 0), M_{i,t})$ to 67 buyers of the policy at time t.

TABLE 4
Bond Parameters

Parameter	Value
Common parameters	
n	3 (years)
δ_1	50th percentile of aggregated losses of all counties across 3 years
δ_2	90th percentile of aggregated losses of all counties across 3 years
c_1	$c_1 = \delta_1$
c_2	$c_2 = \delta_2$
FV	1,000 (million dollars)
P	1,000 (million dollars)
w^R	1,000 (million dollars)
w^I	1,000 (million dollars)
S_0	1,000 (million dollars)
R_{rf}	1,000 (million dollars)
γ^R	0.004
γ^I	0.001
Parameter Set 1	
$D_{i,t}$	10th percentile of losses in county i from time $t-1$ to t
$M_{i,t}$	99th percentile of losses in county i from time $t-1$ to t
Parameter Set 2	
$D_{i,t}$	10th percentile of losses in county i from time $t-1$ to t
$M_{i,t}$	No limit

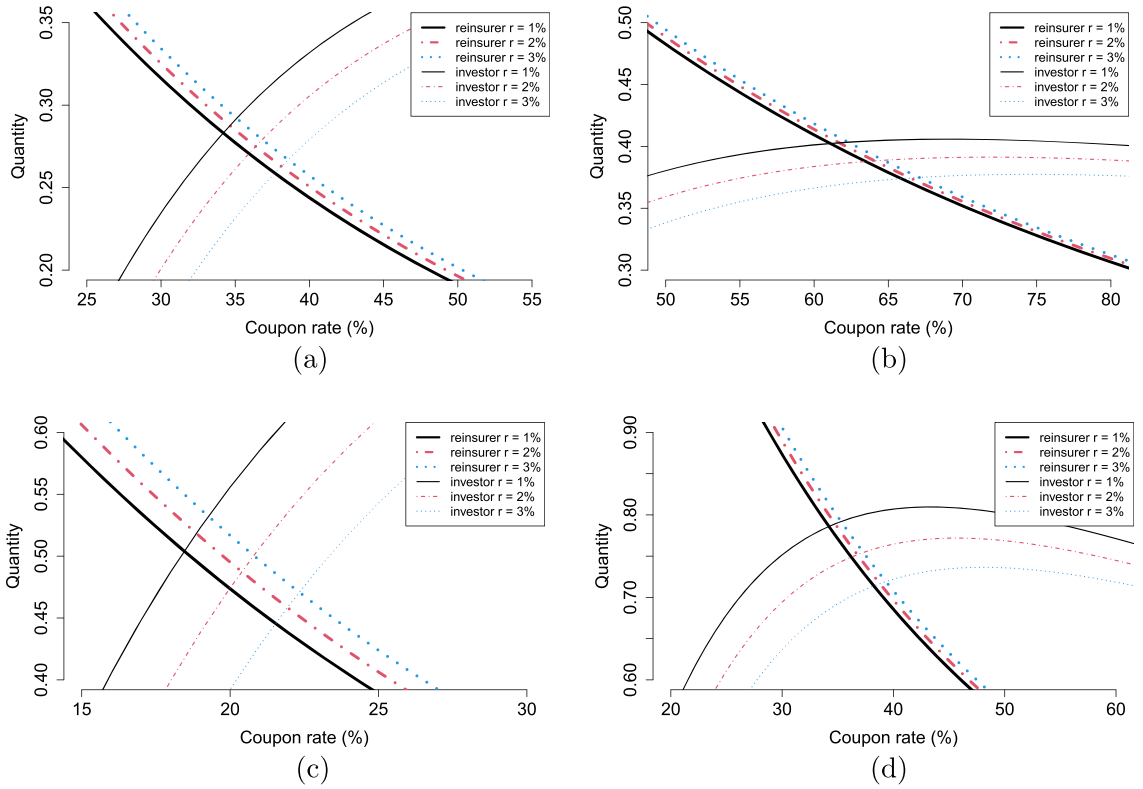


FIGURE 9. Demand and Supply Curves. (a) Parameter Set 1, Binary Reduction; (b) Parameter Set 2, Binary Reduction; (c) Parameter Set 1, Partial Reduction; and (d) Parameter Set 2, Partial Reduction.

Moreover, the CAT index η_t, as listed in Table 1, is the sum of average losses from time $t-1$ to t in each county in Florida: $\eta_t = \sum_{i=1}^{67} L_{i,t}$. Other parameters used for the CAT bond are summarized in Table 4. The trigger levels, δ_1 and δ_2, need to be chosen such that both the reinsurer and the investor are likely to be interested in the bond. If the trigger levels are set too high, it is difficult to reach the triggers and hence for the reinsurer to retain the coupon/principal amount to hedge the storm risk. On the other hand, if the trigger levels are set too low, the risk of losing investment could exceed the investor's risk tolerance. Therefore, the two trigger levels, δ_1 and δ_2, are chosen as the 50th and 90th percentiles of aggregated losses of all counties across 3 years. There is a relatively high probability for the reinsurer to use coupon payments retained for hedging as indicated by δ_1. However, the probability of reaching δ_2—that is, the risk of losing the face values—is much lower. Nevertheless, the trigger levels can be easily modified to cater to investors with different risk appetites. This hedging analysis aims to evaluate the effectiveness of the proposed storm bond in transferring catastrophic risks to the capital market. To accomplish this objective, we examine two different scenarios with varying contract limits. In Parameter Set 1, we set the limit to the 99th percentile of simulated losses in each county over the given period, whereas in Parameter Set 2, we do not impose any contract limit. These two types of reinsurance contracts, which either have a high contract limit or no limit at all, can illustrate how the (re)insurance industry can leverage storm CAT bonds to transfer significant storm losses to the capital market. Moreover, because we are more concerned about extreme losses in the right tail of the storm losses, the deductible amount is less crucial in this setting and hence we do not vary the deductible amount in the two parameter sets. Nonetheless, both the deductible and limit can be easily modified based on a reinsurer's actual contracts.[7]

5.2. Equilibrium Market Price of Risk

Using Equation (18) and Equation (21), we obtain the reinsurer's optimal quantities, θ^R, and investor's optimal quantities, θ^I, at different coupon rates with risk-free rates of 1%, 2%, and 3%. The demand and supply curves, which are represented by quantity against coupon rates, are plotted in Figure 9. Figures 9(a) and 9(b) display demand and supply curves of Parameter Set 1 and Parameter Set 2 for the binary reduction design, respectively. Figures 9(c) and 9(d) display demand and supply curves of Parameter Set 1 and Parameter Set 2 for the partial reduction design, respectively. In all figures, demand curves (from the investor) of different interest rates are more spaced out than supply curves (from the reinsurer). Thus, the investor is more sensitive to interest rates than the reinsurer in general.

The equilibrium quantity, to which both the reinsurer and the investor agree, is the intersection point of the demand and supply curves at a given risk-free rate; that is, $\theta^R = \theta^I$. Equilibrium quantities and their corresponding coupon rates, CP/FV, and market price of risk, λ, are calculated under both Parameter Set 1 and Parameter Set 2 for both binary and partial reduction designs at 1%, 2%, and 3% risk-free rates and are shown in Table 5. Table 5 also summarizes key statistics of the reinsurer's wealth (in million dollars) at the end of the third year with and without hedging at equilibrium quantities. We can see that both λ values and coupon rates are higher under Parameter Set 2 for each bond design. With no policy limit in Parameter Set 2, extreme losses beyond the 99th percentile lead to much larger variation in the reinsurer's wealth, almost doubling the standard deviation before hedging. As a result, the reinsurer is willing to offer a much higher coupon rate and λ to stabilize its cash flows. Furthermore, it is expected to see lower coupon rates under the partial reduction design than those under the binary reduction design because a partial reduction design implies lower risks of losing all coupon or principal amount. We also see higher equilibrium quantities in the partial reduction design under each parameter set and risk-free rate assumption. The market prices of risk, λ, under the linear design are also slightly higher than those under the binary design under each parameter set. On one hand, a partial reduction design can be more attractive to an investor than a binary design due to lower risk embedded; that is, some coupons or principal amount can still be paid even when the trigger level is reached. On the other hand, a partial reduction design is also more desirable from a reinsurer's perspective because the cash flows of the partial reduction design match insurance payouts better; that is, the coupon or principal amounts retained by the reinsurer increase linearly with the size of storm losses as opposed to the binary reduction design. As a result, the partial reduction design achieves a better hedging effectiveness. For example, at 1% risk-free rate, the partial reduction design has 62% and 78% variance reductions under Parameter Set 1 and Parameter Set 2, respectively, whereas the corresponding variance reductions are 53% and 58% in the binary reduction design. Overall, we find that a storm CAT bond with a partial reduction design is more suitable because its coupon rates are more aligned with existing bonds and it is more effective in stabilizing the reinsurer's cash flows. In addition, risk-free rates have little impact on the equilibrium λ and the hedging effectiveness.

[7]Note that in practice, CAT bonds with either per occurrence triggers or annual loss triggers are common. Similarly, the deductible and policy limit of a reinsurance contract can be at either a per occurrence or an aggregated annual level (also called aggregated excess of loss) in practice. In our bond design and pricing, we use the annual level as an example.

TABLE 5
Reinsurer's Wealth (in Million Dollars) at the End of the Third Year with and without Hedging at Equilibrium Quantities and Coupon Rates with Equilibrium λ

Risk-free rate r_f	1%	2%	3%	1%	2%	3%
		Parameter Set 1			Parameter Set 2	
Without hedging						
Mean	1094	1129	1165	1136	1174	1212
SD	311	313	314	575	579	583
Mean-γ^RVariance	707	738	770	–186	–167	–147
Median	1206	1242	1278	1355	1394	1434
95% VaR	1365	1401	1439	1604	1645	1687
99% VaR	1382	1418	1456	1623	1664	1706
With hedging—Binary reduction design						
Coupon rate	34.2%	36.4%	38.6%	61.1%	64.1%	67.1%
Quantity	0.2831	0.2749	0.2669	0.4023	0.3883	0.3749
λ	0.3172	0.3158	0.3146	0.6163	0.6167	0.6174
Mean	1028	1063	1098	882	919	956
SD	213	214	216	368	373	379
Mean-γ^RVariance	847	879	912	340	361	383
Median	1073	1107	1142	914	950	989
95% VaR	1285	1317	1349	1265	1310	1355
99% VaR	1471	1505	1540	1406	1452	1492
Variance reduction	53.2%	53.0%	52.7%	59.0%	58.4%	57.8%
With hedging—Partial reduction design						
Coupon rate	18.5%	20.4%	22.3%	34.2%	36.8%	39.3%
Quantity	0.5041	0.4874	0.4708	0.7860	0.7518	0.7192
λ	0.3351	0.3327	0.3305	0.6440	0.6436	0.6435
Mean	1,016	1,051	1,086	800	837	874
SD	191	191	192	271	278	285
Mean-γ^RVariance	871	904	937	506	528	550
Median	1064	1096	1130	820	854	890
95% VaR	1246	1282	1319	1092	1140	1188
99% VaR	1438	1474	1503	1203	1257	1312
Variance reduction	62.4%	62.5%	62.5%	77.8%	77.0%	76.2%

From the investor's perspective, the storm CAT bond is also attractive because of its high rate of return and high market price of risk, especially for the partial reduction design. The estimated equilibrium λ under Parameter Set 1 (Parameter set 2) is around 0.31 (0.62) with binary reduction design and 0.33 (0.64) with partial reduction design. Galeotti, Gürtler, and Winkelvos (2013) estimated the market price of risk, λ, for CAT bonds to be 0.471 and 0.499 using a reduced dataset and a complete dataset between 1999 and 2009, respectively. In the mortality securities market, the market price of risk ranges from 0.179 to 0.472 (Lin and Cox 2005, 2007; Cairns, Blake, and Dowd 2006; Denuit, Devolder, and Goderniaux 2007). We can see that our estimated λ values are within the reasonable range. Equilibrium λ is comparably higher than similar securities on the market under Parameter Set 2, because the reinsurer transfers all extreme CAT risks to the capital market, implying higher market price of risk. Moreover, Online Appendix G shows the investor's terminal wealth with and without storm CAT bond investment in equilibrium for both bond designs. We can see that there is a significant increase in the expected terminal wealth. Therefore, the proposed storm CAT bond is potentially attractive to investors looking for high returns.

Table 6 presents the equilibrium quantity, coupon rates, and market risk of premium, λ, under the assumption of spatiotemporal independence for the binary and partial reduction designs and the two parameter sets. The equilibrium quantities are consistently lower than those under the spatiotemporal dependence model in Table 5. For example, the equilibrium quantity of the binary reduction design with Parameter Set 2 at 1% interest rate is 0.28 under the independence model, less than half of the

TABLE 6
Equilibrium Quantities, Coupon rates, and λ Assuming Spatiotemporal Independence

Risk-free rate r_f	1%	2%	3%	1%	2%	3%
		Parameter set 1			Parameter set 2	
Binary reduction design						
Coupon rate	34.1%	36.6%	39.1%	51.5%	54.7%	58.1%
Quantity	0.1740	0.1707	0.1675	0.2823	0.2748	0.2674
λ	0.2156	0.2172	0.2188	0.4199	0.4234	0.4270
Partial reduction design						
Coupon rate	14.0%	16.0%	18.1%	22.1%	24.7%	27.2%
Quantity	0.3078	0.3014	0.2945	0.5688	0.5490	0.5295
λ	0.2202	0.2222	0.2245	0.4448	0.4489	0.4533

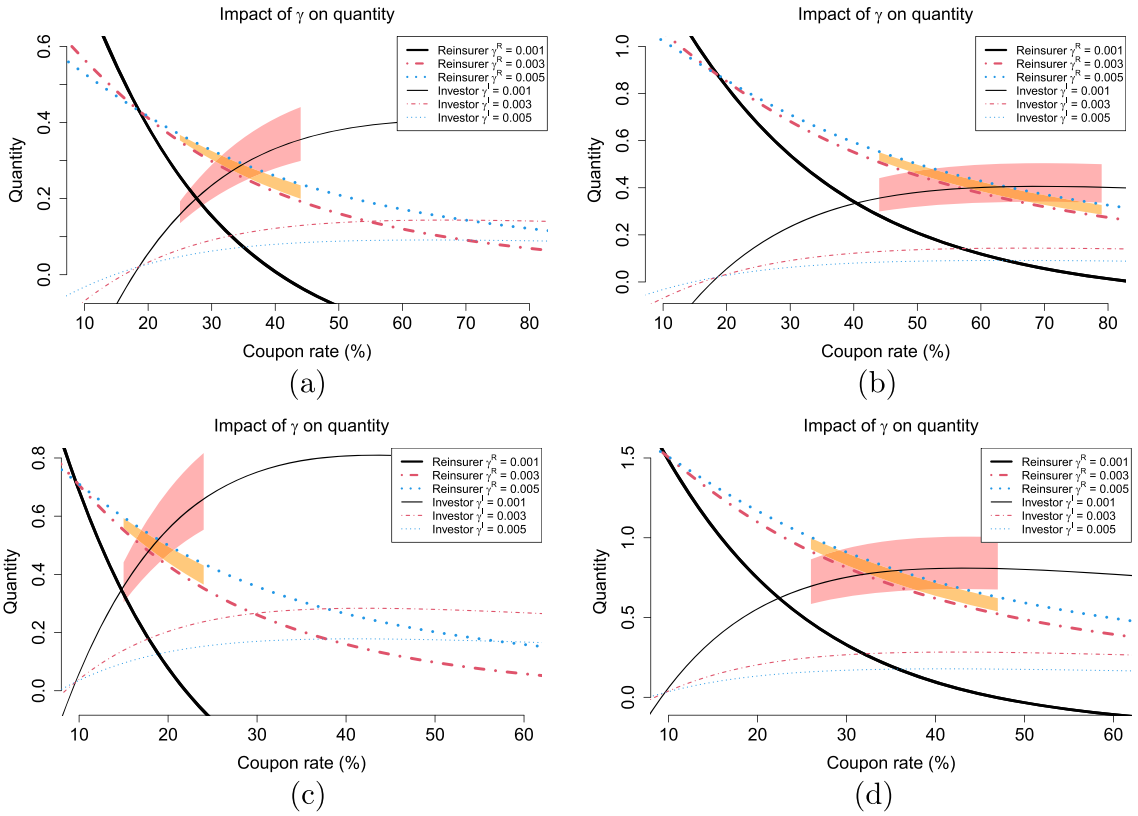


FIGURE 10. Impact of Price Negotiation. The Impact of γ Values on Quantity for (a) Parameter Set 1, Binary Reduction; (b) Parameter Set 2, Binary Reduction; (c) Parameter Set 1, Partial Reduction; and (d) Parameter Set 2, Partial Reduction. *Note:* The shaded region in yellow shows the range of the reinsurer's demand curve with $\gamma^R \in [0.004 \pm 0.0008]$ and the shaded region in pink shows the range of the investor's supply curve with $\gamma^I \in [0.001 \pm 0.0002]$.

quantity (i.e., 0.62) under the dependence model. This shows the significance of dependence modeling in CAT bond design, pricing, and quantity determination. An incorrect assumption of independence will underestimate systemic CAT risks and lead to suboptimal hedging strategies.

5.3. The Impact of Price Negotiation

Previously, we have assumed fixed risk aversion parameters for both the reinsurer (γ^R) and the investor (γ^I). In reality, however, both parameters can vary and this leads to room for price negotiation between the two parties. In this subsection, we

discuss the impact of price negotiation. We assume that γ^R and γ^I can range around 20% of the previous baseline values; that is, $\gamma^R \in [0.004 \pm 0.0008]$ and $\gamma^I \in [0.001 \pm 0.0002]$. Figure 10 displays the equilibrium results. Because the impact of risk-free rates is very small, for illustration purposes we only show results for a risk-free rate of 1%. For each plot, the pink shaded region shows the range of the investor's supply curve, and the yellow shaded region shows the range of the reinsurer's demand curve. The intersections of the two shaded regions yield an optimal range of quantity and price that allows negotiation. For example, for the partial reduction design under Parameter Set 1, the intersection of the shaded regions gives an equilibrium quantity ranging from 0.45 to 0.55 and an equilibrium coupon rate ranging from 16% to 21%. Any prices and quantities within these ranges are acceptable to the reinsurer and the investor, and the final result is then subject to their bargaining power.

Figure 10 also illustrates the impact of risk aversion parameters. We can see that when parameter values increase, both demand and supply curves become flatter; that is, the magnitudes of the gradient decrease. At a given γ^R value of the reinsurer, a higher γ^I (i.e., a higher level of risk aversion of the investor) leads to a lower equilibrium quantity and a higher equilibrium coupon rate, indicating the investor's need for higher compensation for its investment risk. On the other hand, at a given γ^I value of the investor, a higher γ^R (i.e., a higher level of risk aversion of the reinsurer) leads to a higher equilibrium quantity and a higher equilibrium coupon rate, indicating the reinsurer's stronger desire for hedging.

6. DISCUSSION AND CONCLUSION

Both the frequency and intensity of natural catastrophes, especially weather-related events such as storms and floods, have been increasing due to climate change in recent years. This leads to rising storm CAT risks the property and casualty insurance industry faces. Researchers have shown that various reasons, including market imperfections and price regulations, limit sufficient CAT risk diversification in the insurance industry. As a result, potential insolvencies of insurers and reinsurers remain a problem if CAT risks are not further diversified. To address this issue, we propose an index-based storm CAT bond for reinsurers to hedge risks related to storm losses with both a binary reduction design and a partial reduction design in this article. Both coupon and principal payments are contingent on storm events during the bond's term to maturity. We refine the multivariate statistical modeling of high-dimensional storm risks by proposing a general 2PAR distribution for the margin and a semicontinuous spatiotemporal copula for the dependence structure. The proposed statistical framework addresses the technical challenges in modeling spatially dependent catastrophe storm loss data with a large proportion of zero values and potentially heavy-tailed right-skewed positive losses. We also endogenously determine the equilibrium market price of risk by considering the strategic interaction between the bond issuer and investors. Our empirical results show that the variance of the reinsurer's wealth upon maturity of the bond is reduced by up to 60% after hedging with the binary design and up to 78% with the partial reduction design. Therefore, the proposed bond can effectively stabilize the reinsurer's cash flow. Moreover, the proposed bond offers high market prices of risk at equilibrium, which can be very attractive to investors because of the potentially high returns. In addition, we find the partial reduction design of the storm CAT bond more suitable from both the reinsurer's and investor's perspectives, because it leads to more effective hedging results for the reinsurer and offers higher market prices of risk for the investor. Though this article focuses on storm risk, the proposed modeling and valuation framework can be easily applied to other CAT bond products.

DISCLOSURE STATEMENT

No potential conflict of interest was reported by the author(s).

FUNDING

SH acknowledges financial support from the Society of Actuaries James C. Hickman Scholar Program, Spencer Educational Foundation, and Wisconsin School of Business, University of Wisconsin–Madison. JZ acknowledges funding from the Singapore Ministry of Education Academic Research Fund Tier 1 (RG55/20). WZ acknowledges funding from the Singapore Ministry of Education Academic Research Fund Tier 1 (RG143/19) and the Society of Actuaries Education Institution Grant.

REFERENCES

Aas, K., C. Czado, A. Frigessi, and H. Bakken. 2009. Pair-copula constructions of multiple dependence. *Insurance: Mathematics and Economics* 44 (2): 182–98. doi:10.1016/j.insmatheco.2007.02.001

Aitchison, J. 1955. On the distribution of a positive random variable having a discrete probability mass at the origin. *Journal of the American Statistical Association* 50 (271):901–8.

Aon. 2021. Weather, climate & catastrophe insight. https://www.aon.com/weatherclimate-catastrophe/index.html

Bakshi, G., and D. Madan. 2002. Average rate claims with emphasis on catastrophe loss options. *The Journal of Financial and Quantitative Analysis* 37 (1): 93–115. doi:10.2307/3594996

Bantwal, V. J., and H. C. Kunreuther. 2000. A CAT bond premium puzzle? *Journal of Psychology and Financial Markets* 1 (1):76–91. doi:10.1207/S15327760JPFM0101_07

Bedford, T., and R. M. Cooke. 2002. Vines—A new graphical model for dependent random variables. *Annals of Statistics* 30 (4):1031–68.

Braun, A. 2011. Pricing catastrophe swaps: A contingent claims approach. *Insurance: Mathematics and Economics* 49 (3):520–36. doi:10.1016/j.insmatheco.2011.08.003

Braun, A. 2016. Pricing in the primary market for CAT bonds: New empirical evidence. *Journal of Risk and Insurance* 83 (4):811–47. doi:10.1111/jori.12067

Braun, A., and C. Kousky. 2021. *Catastrophe bonds*. Wharton Risk Center Primer.

Burnecki, K., G. Kukla, and R. Weron. 2000. Property insurance loss distributions. *Physica A: Statistical Mechanics and Its Applications* 287 (1):269–78. doi:10.1016/S0378-4371(00)00453-2

Cairns, A. J. G., D. Blake, and K. Dowd. 2006. A two-factor model for stochastic mortality with parameter uncertainty: Theory and calibration. *Journal of Risk and Insurance* 73 (4):687–718. doi:10.1111/j.1539-6975.2006.00195.x

Campbell, S. D., and F. X. Diebold. 2005. Weather forecasting for weather derivatives. *Journal of the American Statistical Association* 100 (469):6–16. doi:10.1198/016214504000001051

Canter, M. S., J. B. Cole, and R. L. Sandor. 1996. Insurance derivatives: A new asset class for the capital markets and a new hedging tool for the insurance industry. *Journal of Derivatives* 4 (2):89–104. doi:10.3905/jod.1996.407966

Charpentier, A. 2008. Insurability of climate risks. *Geneva Papers on Risk and Insurance: Issues and Practice* 33:91–109. doi:10.1057/palgrave.gpp.2510155

Chen, H., and S. H. Cox. 2009. Modeling mortality with jumps: Applications to mortality securitization. *The Journal of Risk and Insurance* 76 (3):727–51. doi:10.1111/j.1539-6975.2009.01313.x

Chen, H., and J. D. Cummins. 2010. Longevity bond premiums: The extreme value approach and risk cubic pricing. *Insurance: Mathematics and Economics* 46 (1):150–61. doi:10.1016/j.insmatheco.2009.09.007

Coronese, M., F. Lamperti, K. Keller, F. Chiaromonte, and A. Roventini. 2019. Evidence for sharp increase in the economic damages of extreme natural disasters. *Proceedings of the National Academy of Sciences of the United States of America* 116 (43):21450–55. doi:10.1073/pnas.1907826116

Cossette, H., E. Marceau, and F. Marri. 2008. On the compound Poisson risk model with dependence based on a generalized Farlie-Gumbel-Morgenstern copula. *Insurance: Mathematics and Economics* 43 (3):444–55. doi:10.1016/j.insmatheco.2008.08.009

Cox, S. H., J. R. Fairchild, and H. W. Pedersen. 2000. Economic aspects of securitization of risk. *ASTIN Bulletin* 30 (1):157–93. doi:10.2143/AST.30.1.504631

Cox, S. H., and H. W. Pedersen. 2000. Catastrophe risk bonds. *North American Actuarial Journal* 4 (4):56–82. doi:10.1080/10920277.2000.10595938

Cummins, J. D. 2008. CAT bond and other risk-linked securities: State of the market and recent developments. *Risk Management and Insurance Review* 11 (1):23–47. doi:10.1111/j.1540-6296.2008.00127.x

Cummins, J. D., N. Doherty, and A. Lo. 2002. Can insurers pay for the "big one"? Measuring the capacity of the insurance market to respond to catastrophic losses. *Journal of Banking & Finance* 26 (2–3):557–83. doi:10.1016/S0378-4266(01)00234-5

Cummins, J. D., and H. Geman. 1995. Pricing catastrophe insurance futures and call spreads: An arbitrage approach. *The Journal of Fixed Income* 4 (4):46–57. doi:10.3905/jfi.1995.408128

Cummins, J. D., D. Lalonde, and R. D. Phillips. 2004. The basis risk of catastrophic-loss index securities. *Journal of Financial Economics* 71 (1):77–111. doi:10.1016/S0304-405X(03)00172-7

Cummins, J. D., and P. Trainar. 2009. Securitization, insurance, and reinsurance. *Journal of Risk and Insurance* 76:463–92. doi:10.1111/j.1539-6975.2009.01319.x

Dassios, A., and J.-W. Jang. 2003. Pricing of catastrophe reinsurance and derivatives using the Cox process with shot noise intensity. *Finance and Stochastics* 7 (1):73–95. doi:10.1007/s007800200079

Denuit, M., P. Devolder, and A.-C. Goderniaux. 2007. Securitization of longevity risk: Pricing survivor bonds with Wang transform in the Lee-Carter framework. *Journal of Risk and Insurance* 74 (1):87–113. doi:10.1111/j.1539-6975.2007.00203.x

Doherty, N. A. 1997. Financial innovation in the management of catastrophe risk. *Journal of Applied Corporate Finance* 10:84–95. doi:10.1111/j.1745-6622.1997.tb00149.x

Dowd, K., D. Blake, A. J. Cairns, and P. Dawson. 2006. Survivor swaps. *Journal of Risk and Insurance* 73 (1):1–17. doi:10.1111/j.1539-6975.2006.00163.x

Duan, N., W. G. Manning, C. N. Morris, and J. P. Newhouse. 1983. A comparison of alternative models for the demand for medical care. *Journal of Business & Economic Statistics* 1 (2):115–26.

Dunstone, N. J., D. M. Smith, B. B. B. Booth, L. Hermanson, and R. Eade. 2013. Anthropogenic aerosol forcing of Atlantic tropical storms. *Nature Geoscience* 6 (7):534–39. doi:10.1038/ngeo1854

Egami, M., and V. R. Young. 2008. Indifference prices of structured catastrophe (CAT) bonds. *Insurance: Mathematics and Economics* 42 (2):771–78. doi:10.1016/j.insmatheco.2007.08.004

Erhardt, T. M., C. Czado, and U. Schepsmeier. 2015a. R-vine models for spatial time series with an application to daily mean temperature. *Biometrics* 71 (2):323–32. doi:10.1111/biom.12279

Erhardt, T. M., C. Czado, and U. Schepsmeier. 2015b. Spatial composite likelihood inference using local C-vines. *Journal of Multivariate Analysis* 138:74–88. doi:10.1016/j.jmva.2015.01.021

Evans, S. 2022. Cat bond market supply–demand mismatch persists as pipeline builds. Last accessed August 28, 2023. https://www.artemis.bm/news/cat-bond-market-supply-demand-mismatch-persists-as-pipeline-builds/#:~:text=Cat%20bond%20market%20supply%2Ddemand%20mismatch%20persists%20as%20pipeline%20builds,-11th%20May%202022&text=The%20mismatch%20between%20supply%20and,bond%20deals%20continues%20to%20expand.

Frees, E. W., and E. A. Valdez. 1998. Understanding relationships using copulas. *North American Actuarial Journal* 2 (1):1–25. doi:10.1080/10920277.1998.10595667

Frees, E. W., and E. A. Valdez. 2008. Hierarchical insurance claims modeling. *Journal of the American Statistical Association* 103 (484):1457–69. doi:10.1198/016214508000000823

Frees, E. W., and P. Wang. 2005. Credibility using copulas. *North American Actuarial Journal* 9 (2):31–48. doi:10.1080/10920277.2005.10596196

Froot, K. A. 1999. The evolving market for catastrophic event risk the distribution of catastrophic event risk. *Risk Management and lnsurance Review* 2 (3): 1–28. doi:10.1111/j.1540-6296.1999.tb00001.x

Froot, K. A. 2001. The market for catastrophe risk: A clinical examination. *Journal of Financial Economics* 60 (2–3):529–71. doi:10.1016/S0304-405X(01)00052-6

Froot, K. A., B. Murphy, A. Stern, and S. Usher. 1995. The emerging asset class: Insurance risk. *Viewpoint* 24 (3):19–28.

Galeotti, M., M. Gürtler, and C. Winkelvos. 2013. Accuracy of premium calculation models for CAT bonds—An empirical analysis. *Journal of Risk and Insurance* 80 (2):401–21. doi:10.1111/j.1539-6975.2012.01482.x

Genest, C., B. Rémillard, and D. Beaudoin. 2009. Goodness-of-fit tests for copulas: A review and a power study. *Insurance: Mathematics and Economics* 44 (2):199–213. doi:10.1016/j.insmatheco.2007.10.005

Golden, L. L., M. Wang, and C. Yang. 2007. Handling weather related risks through the financial markets: Considerations of credit risk, basis risk, and hedging. *Journal of Risk and Insurance* 74 (2):319–46. doi:10.1111/j.1539-6975.2007.00215.x

Götze, T., and M. Gürtler. 2020. Hard markets, hard times: On the inefficiency of the CAT bond market. *Journal of Corporate Finance* 62:101553. doi:10.1016/j.jcorpfin.2019.101553

Götze, T., and M. Gürtler. 2022. Risk transfer beyond reinsurance: The added value of CAT bonds. *Geneva Papers on Risk and Insurance: Issues and Practice* 47 (1):125–71. doi:10.1057/s41288-021-00234-6

Gräler, B. 2013. spcopula: Modelling spatial and spatio-temporal dependence with copulas in R. http://ben.graeler.org/spatial-copulas/l.

Gräler, B. 2014. Modelling skewed spatial random fields through the spatial vine copula. *Spatial Statistics* 10:87–102. doi:10.1016/j.spasta.2014.01.001

Gräler, B., and E. Pebesma. 2012. Modelling dependence in space and time with vine copulas. Paper presented at the Ninth International Geostatistics Congress, Oslo, Norway, June 11–15, 2012.

Gürtler, M., M. Hibbeln, and C. Winkelvos. 2016. The impact of the financial crisis and natural catastrophes on CAT bonds. *Journal of Risk and Insurance* 83 (3):579–612. doi:10.1111/jori.12057

Hodges, S. D., and A. Neuberger. 1989. Optimal replication of contingent claims under transaction costs. *Review of Futures Markets* 8 (2):223–38.

Hoeppe, P. 2016. Trends in weather related disasters—Consequences for insurers and society. *Weather and Climate Extremes* 11:70–79. doi:10.1016/j.wace.2015.10.002

Ibragimov, R., D. Jaffee, and J. Walden. 2009. Nondiversification traps in catastrophe insurance markets. *Review of Financial Studies* 22 (3):959–93. doi:10.1093/rfs/hhn021

Jaimungal, S., and T. Wang. 2006. Catastrophe options with stochastic interest rates and compound Poisson losses. *Insurance: Mathematics and Economics* 38 (3):469–83. doi:10.1016/j.insmatheco.2005.11.008

Jarrow, R. A. 2010. A simple robust model for CAT bond valuation. *Finance Research Letters* 7 (2):72–79. doi:10.1016/j.frl.2010.02.005

Joe, H., and J. J. Xu. 1996. The estimation method of inference functions for margins for multivariate models. Technical Report no. 166, Department of Statistics, University of British Columbia.

Juri, A., and M. V. Ẅuthrich. 2002. Copula convergence theorems for tail events. *Insurance: Mathematics and Economics* 30 (3):405–20. doi:10.1016/S0167-6687(02)00121-X

Karagiannis, N., H. Assa, A. A. Pantelous, and C. G. Turvey. 2016. Modelling and pricing of catastrophe risk bonds with a temperature-based agricultural application. *Quantitative Finance* 16 (12):1949–59. doi:10.1080/14697688.2016.1211791

Klugman, S. A., and R. Parsa. 1999. Fitting bivariate loss distributions with copulas. *Insurance: Mathematics and Economics* 24 (1–2):139–48. doi:10.1016/S0167-6687(98)00039-0

Krupskii, P., and M. G. Genton. 2017. Factor copula models for data with spatio-temporal dependence. *Spatial Statistics* 22:180–95. doi:10.1016/j.spasta.2017.10.001

Krupskii, P., R. Huser, and M. G. Genton. 2018. Factor copula models for replicated spatial data. *Journal of the American Statistical Association* 113 (521): 467–79. doi:10.1080/01621459.2016.1261712

Kurowicka, D., and R. Cooke. 2006. *Uncertainty analysis with high dimensional dependence modelling*. John Wiley and Sons.

Lee, J. P., and M. T. Yu. 2002. Pricing default-risky CAT bonds with moral hazard and basis risk. *Journal of Risk and Insurance* 69 (1):25–44. doi:10.1111/1539-6975.00003

Lee, J. P., and M. T. Yu. 2007. Valuation of catastrophe reinsurance with catastrophe bonds. *Insurance: Mathematics and Economics* 41 (2):264–78. doi:10.1016/j.insmatheco.2006.11.003

Levi, C., and C. Partrat. 1991. Statistical analysis of natural events in the United States. *ASTIN Bulletin* 21 (2):253–76. doi:10.1017/S051503610000458X

Li, Z., J. Beirlant, and S. Meng. 2021. Generalizing the log-Moyal distribution and regression models for heavy-tailed loss data. *ASTIN Bulletin* 51 (1):57–99. doi:10.1017/asb.2020.35

Lin, Y., and S. H. Cox. 2005. Securitization of mortality risks in life annuities. *Journal of Risk and Insurance* 72 (2):227–52. doi:10.1111/j.1539-6975.2005.00122.x

Lin, Y., and S. H. Cox. 2007. Natural hedging of life and annuity mortality risks. *North American Actuarial Journal* 11 (3):1–15. doi:10.1080/10920277.2007.10597464

Lin, Y., and S. H. Cox. 2008. Securitization of catastrophe mortality risks. *Insurance: Mathematics and Economics* 42 (2):628–37. doi:10.1016/j.insmatheco.2007.06.005

Manning, W. G., C. N. Morris, J. P. Newhouse, L. L. Orr, N. Duan, E. B. Keeler, A. Leibowitz, K. H. Marquis, M. S. Marquis, and C. E. Phelps. 1981. A two-part model of the demand for medical care: Preliminary results from the Health Insurance Study. *Health, Economics, and Health Economics* 137: 103–23.

McNeil, A. J., R. Frey, and P. Embrechts. 2015. *Quantitative risk management: Concepts, techniques and tools*—Revised edition. Princeton University Press.

Milidonis, A., and M. F. Grace. 2008. Tax-deductible pre-event catastrophe loss reserves: The case of Florida. *ASTIN Bulletin* 38 (1):13–51. doi:10.2143/AST.38.1.2030401

Mills, E. 2005. Insurance in a climate of change. *Science* 309 (5737):1040–44. doi:10.1126/science.1112121

Muermann, A. 2008. Market price of insurance risk implied by catastrophe derivatives. *North American Actuarial Journal* 12 (3):221–27. doi:10.1080/10920277.2008.10597518

Murakami, H., T. L. Delworth, W. F. Cooke, M. Zhao, B. Xiang, and P.-C. Hsu. 2020. Detected climatic change in global distribution of tropical cyclones. *Proceedings of the National Academy of Sciences* 117 (20):10706–14. doi:10.1073/pnas.1922500117

Myhre, G., K. Alterskjar, C. W. Stjern Hodnebrog, L. Marelle, B. H. Samset, J. Sillmann, N. Schaller, E. Fischer, M. Schulz, and A. Stohl. 2019. Frequency of extreme precipitation increases extensively with event rareness under global warming. *Scientific Reports* 9 (1):2–11. doi:10.1038/s41598-019-52277-4

Nell, M., and A. Richter. 2004. Improving risk allocation through indexed CAT bonds. *Geneva Papers on Risk and Insurance* 29 (2):183–201. doi:10.1111/j.1468-0440.2004.00281.x

Nelsen, R. B. 2007. *An introduction to copulas*. 2nd ed. Springer Science & Business Media.

Niehaus, G. 2002. The allocation of catastrophe risk. *Journal of Banking & Finance* 26:585–96. doi:10.1016/S0378-4266(01)00235-7

Nowak, P., and M. Romaniuk. 2013. Pricing and simulations of catastrophe bonds. *Insurance: Mathematics and Economics* 52 (1):18–28. doi:10.1016/j.insmatheco.2012.10.006

Odening, M., and Z. Shen. 2012. Challenges of insuring weather risk in agriculture. *Agricultural Finance Review* 74 (2):188–99. doi:10.1108/AFR-11-2013-0039

Okhrin, O., M. Odening, and W. Xu. 2013. Systemic weather risk and crop insurance: The case of China. *Journal of Risk and Insurance* 80 (2):351–72. doi:10.1111/j.1539-6975.2012.01476.x

Panagiotelis, A., C. Czado, H. Joe, and J. Stöber. 2017. Model selection for discrete regular vine copulas. *Computational Statistics & Data Analysis* 106:138–52. doi:10.1016/j.csda.2016.09.007

Pitt, D., S. Trück, R. van den Honert, and W. W. Wong. 2020. Modeling risks from natural hazards with generalized additive models for location, scale and shape. *Journal of Environmental Management* 275:111075. doi:10.1016/j.jenvman.2020.111075

Priest, G. L. 1996. The government, the market, and the problem of catastrophic loss. *Journal of Risk and Uncertainty* 12 (2–3):219–37. doi:10.1007/BF00055795

Shi, P., X. Feng, and J.-P. Boucher. 2016. Multilevel modeling of insurance claims using copulas. *The Annals of Applied Statistics* 10 (2):834–63. doi:10.1214/16-AOAS914

Shi, P., and G. Y. Lee. 2022. Copula regression for compound distributions with endogenous covariates with applications in insurance deductible pricing. *Journal of the American Statistical Association* 117 (539):1094–109. doi:10.1080/01621459.2022.2040519

Shi, P., and L. Yang. 2018. Pair copula constructions for insurance experience rating. *Journal of the American Statistical Association* 113 (521):122–33. doi:10.1080/01621459.2017.1330692

Su, J., and L. Hua. 2017. A general approach to full-range tail dependence copulas. *Insurance: Mathematics and Economics* 77:49–64. doi:10.1016/j.insmatheco.2017.08.009

Swiss Re Institute. 2021. Natural catastrophes in 2020: Secondary perils in the spotlight, but don't forget primary-peril risks. https://www.swissre.com/dam/jcr:ebd39a3b-dc55-4b34-9246-6dd8e5715c8b/sigma-1-2021-en.pdf

Tang, Q., and Z. Yuan. 2019. CAT bond pricing under a product probability measure with pot risk characterization. *ASTIN Bulletin* 49 (2):457–90. doi:10.1017/asb.2019.11

Vaugirard, V. E. 2003. Pricing catastrophe bonds by an arbitrage approach. *Quarterly Review of Economics and Finance* 43:119–32. doi:10.1016/S1062-9769(02)00158-8

Wang, G., and X. Wang. 2019. Catastrophe option pricing with auto-correlated and catastrophe-dependent intensity. *Physica A: Statistical Mechanics and Its Applications* 526:1–12. doi:10.1016/j.physa.2019.04.045

Wang, S. S. 1996. Premium calculation by transforming the layer premium density. *ASTIN Bulletin* 26 (1):71–92. doi:10.2143/AST.26.1.563234

Wang, S. S. 2000. A class of distortion operators for pricing financial and insurance risks. *Journal of Risk and Insurance* 67 (1):15–36. doi:10.2307/253675

Wang, S. S. 2002. A universal framework for pricing financial and insurance risks. *ASTIN Bulletin* 32 (2):213–34. doi:10.2143/AST.32.2.1027

Wang, X. 2019. Valuation of new-designed contracts for catastrophe risk management. *North American Journal of Economics and Finance* 50:1–8.

Wang, Y., T. Wang, and J. Zhuang. 2018. Modeling continuous time series with many zeros and an application to earthquakes. *Environmetrics* 29 (4):1–21. doi:10.1002/env.2500

Young, V. R. 2004. Pricing in an incomplete market with an affine term structure. *Mathematical Finance* 14 (3):359–81. doi:10.1111/j.0960-1627.2004.00195.x

Zhao, Z., P. Shi, and X. Feng. 2021. Knowledge learning of insurance risks using dependence models. *INFORMS Journal on Computing* 33 (3):1177–96. doi:10.1287/ijoc.2020.1005

Zhou, R., and M. Ji. 2021. Modelling mortality dependence: An application of dynamic vine copula. *Insurance: Mathematics and Economics* 99:241–55. doi:10.1016/j.insmatheco.2021.03.022

Zhu, W., K. S. Tan, L. Porth, and C.-W. Wang. 2018. Spatial dependence and aggregation in weather risk hedging: A Lévy subordinated hierarchical Archimedean copulas (LSHAC) approach. *ASTIN Bulletin* 48 (2):779–815. doi:10.1017/asb.2018.6

Zhu, W., K. S. Tan, and C.-W. Wang. 2017. Modeling multicountry longevity risk with mortality dependence: A Lévy subordinated hierarchical Archimedean copulas approach. *Journal of Risk and Insurance* 84 (Suppl. 1):477–93. doi:10.1111/jori.12198

Discussions on this article can be submitted until April 1, 2024. The authors reserve the right to reply to any discussion. Please see the Instructions for Authors found online at http://www.tandfonline.com/uaaj for submission instructions.